

South Australia

mesa

journal



MESA Journal 88
2018 – Issue 3



Government of South Australia
Department for Energy and Mining

www.energymining.sa.gov.au/mesa_journal

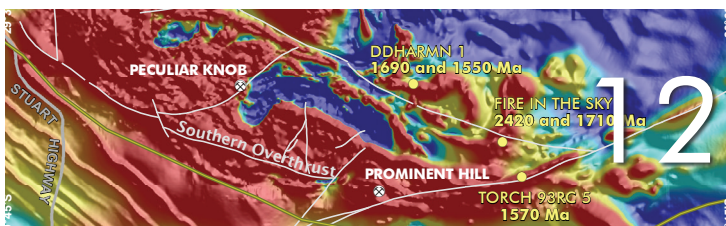
Are *YOU* ready for **GDA2020?**

- Australia is moving to a new official datum – GDA2020.
- South Australian Government agencies are transitioning to GDA2020 during the first quarter of 2019.
- Mining and exploration policies and guidelines will be updated.
- If necessary, update your software and systems to use or supply data in GDA2020.
- Visit www.icsm.gov.au

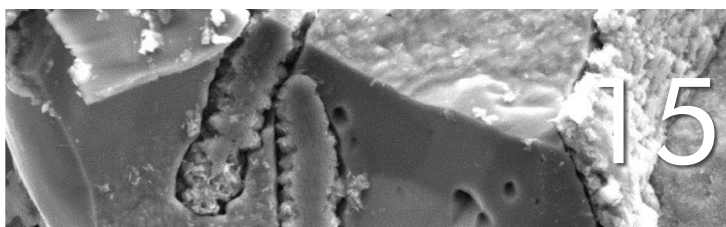
www.energymining.sa.gov.au/gda2020



The final event in the long evolution of the Gawler Craton: new constraints on 1450 Ma metamorphism and magmatism – *Laura Morrissey, Karin Barovich, Martin Hand, Katherine Howard, Justin Payne and Anthony Reid*



Source to Spectrum: project update – *Justin Payne, Tom Raimondo, Laura Morrissey, Martin Hand, Richard Lilly, Andrew Tomkins, Anthony Reid, Rian Dutch, Claire Wade, Jonathan Hamisi, Mitchell Bockmann and Matthew Janicki*



Spectral analysis of drill core from the Kanmantoo copper deposit – *Alan Mauger, John Keeling, Peter Rolley and Hayden Arbon*



Building the Coompana Province – *Tom Wise, Rian Dutch, Mark Pawley, Clive Foss and Stephan Thiel*

Inquiries

MESA Journal Manager,
Department for Energy and Mining
GPO Box 320, Adelaide SA 5001
11 Waymouth Street, Adelaide SA
Phone: +61 8 8463 3000
DEM.MesaJournal@sa.gov.au

205092

ISSN 2207-2152

Subscriptions

Subscribe online. Subscription is free and notification is via regular email alerts directly linking you to the online copy.

Contributions

Contributions are invited provided they are relevant to South Australia and relate to the geosciences or mineral and energy resources. Technical articles are peer reviewed.

Back issues

Back issues are available online. Previous articles can also be searched for and downloaded via SARIG.

© Government of South Australia Disclaimer

Although all reasonable care has been taken in the preparation and compilation of the information in the MESA Journal, it has been provided in good faith for general information only and does not purport to be professional advice. No warranty,

express or implied, is given as to the completeness, correctness, accuracy, reliability or currency of the materials. DEM and the Crown in the right of the state of South Australia do not accept responsibility for and will not be held liable to any recipient of the information for any loss or damage however caused (including negligence) which may be directly or indirectly suffered as a consequence of use of these materials. DEM reserves the right to update, amend or supplement the information from time to time at its discretion.

Warning

Aboriginal and Torres Strait Islanders are warned that this publication may contain images and names of deceased persons.

Cover

Kanmantoo copper mine, 2018, looking northerly showing main open cut (right) with haul road access to Kavanagh and Spitfire ore bodies. Stockpile of low-grade copper ore and waste rock dump (centre and upper left) with remains of the historic Paringa copper mine Cornish beam engine house (1870 and 1912) in the centre foreground. See article on Kanmantoo spectral analysis on pp. 15–24. (Courtesy Hillgrove Resources; photo 416794)

The final event in the long evolution of the Gawler Craton: new constraints on 1450 Ma metamorphism and magmatism

Laura Morrissey^{1, 2}, Karin Barovich², Martin Hand², Katherine Howard², Justin Payne¹ and Anthony Reid³

¹ School of Natural and Built Environments, University of South Australia

² School of Physical Sciences, University of Adelaide

³ Geological Survey of South Australia, Department for Energy and Mining

Introduction

Potential field data across the northern Gawler Craton reveal structural fabrics and a number of large plutonic bodies that suggest the region has a complex tectono-metamorphic and magmatic evolution (Fig. 1). Existing geochronological studies confirm this complex history, with multiple phases of magmatism between c. 2530–1750 Ma (Howard et al. 2011; Reid et al. 2014) and the recognition of at least three high temperature metamorphic events at 1730–1685 Ma, 1600–1580 Ma and c. 1520 Ma (Payne et al. 2008; Cutts, Hand and Kelsey 2011; Reid et al. 2014). Mineral and petroleum exploration drillholes into some of the structural features of the region to the northwest of the Mabel Creek Ridge recovered gneissic rocks with migmatitic rock textures as well as undeformed granite (Figs 1, 2). Interpreted basement geological maps of the northern Gawler Craton previously attributed these granitic rocks to the c. 1600–1570 Ma Hiltaba Suite (Fairclough, Schwarz and Ferris 2003; Howard et al. 2011), therefore extending the footprint of Hiltaba Suite magmatism across the whole Gawler Craton.

Recent work conducted as part of the Source to Spectrum Australian Research Council (ARC) Linkage Project (Payne et al. 2018) has revealed that at least three drillholes in the northern Gawler Craton record metamorphism and magmatism at 1463–1444 Ma, and that the granite bodies are part of a distinct, c. 1450 Ma thermal event rather than part of the Hiltaba Suite (Morrissey et al. in press). Here, we provide an overview of the results published in our open access article in *Geoscience Frontiers* (Morrissey et al. in press), with a focus on the significance of this event for the Gawler Craton.

Geology of the northern Gawler Craton

The poorly exposed northern Gawler Craton comprises four geophysically defined domains, the Peak and Denison Inlier, the Mount Woods Domain, Coober Pedy Ridge and the Nawa Domain (Fig. 1). These domains are separated from the Mulgathing Complex in the central Gawler Craton by the crustal-scale Karari Shear Zone (Fig. 1). The drillholes containing c. 1450 Ma magmatic and metamorphic rocks are from the Nawa Domain (Fig. 1). The Nawa Domain is the northernmost domain of the Gawler Craton and is almost entirely under cover. As a result, the basement geology is inferred from sparse drillholes and geophysics. Lithologies intersected in drill core in the Nawa Domain include orthogneiss with magmatic crystallisation ages of c. 2530 Ma (Reid et al. 2014) and 1780–1750 Ma (Howard et al. 2011) and metasedimentary rocks deposited between 1740–1720 Ma (Payne, Barovich and Hand 2006). The Nawa Domain predominantly records Kimban Orogeny aged metamorphism (c. 1730–1690 Ma; Payne et al. 2008; Howard et al. 2011; Reid et al. 2014). High-grade reworking of the southern Nawa Domain occurred at c. 1600–1550 Ma (Payne et al. 2008; Cutts, Hand and Kelsey 2011) and one drillhole (GOMA 4; Fig. 1) also provides enigmatic evidence for metamorphism at c. 1520 Ma (Reid et al. 2014).

Drillholes sampled: rock types and analyses conducted

Three diamond drillholes were sampled as part of the Morrissey et al. (in press) study (Table 1). Drillhole OBD 09 intersected strongly foliated

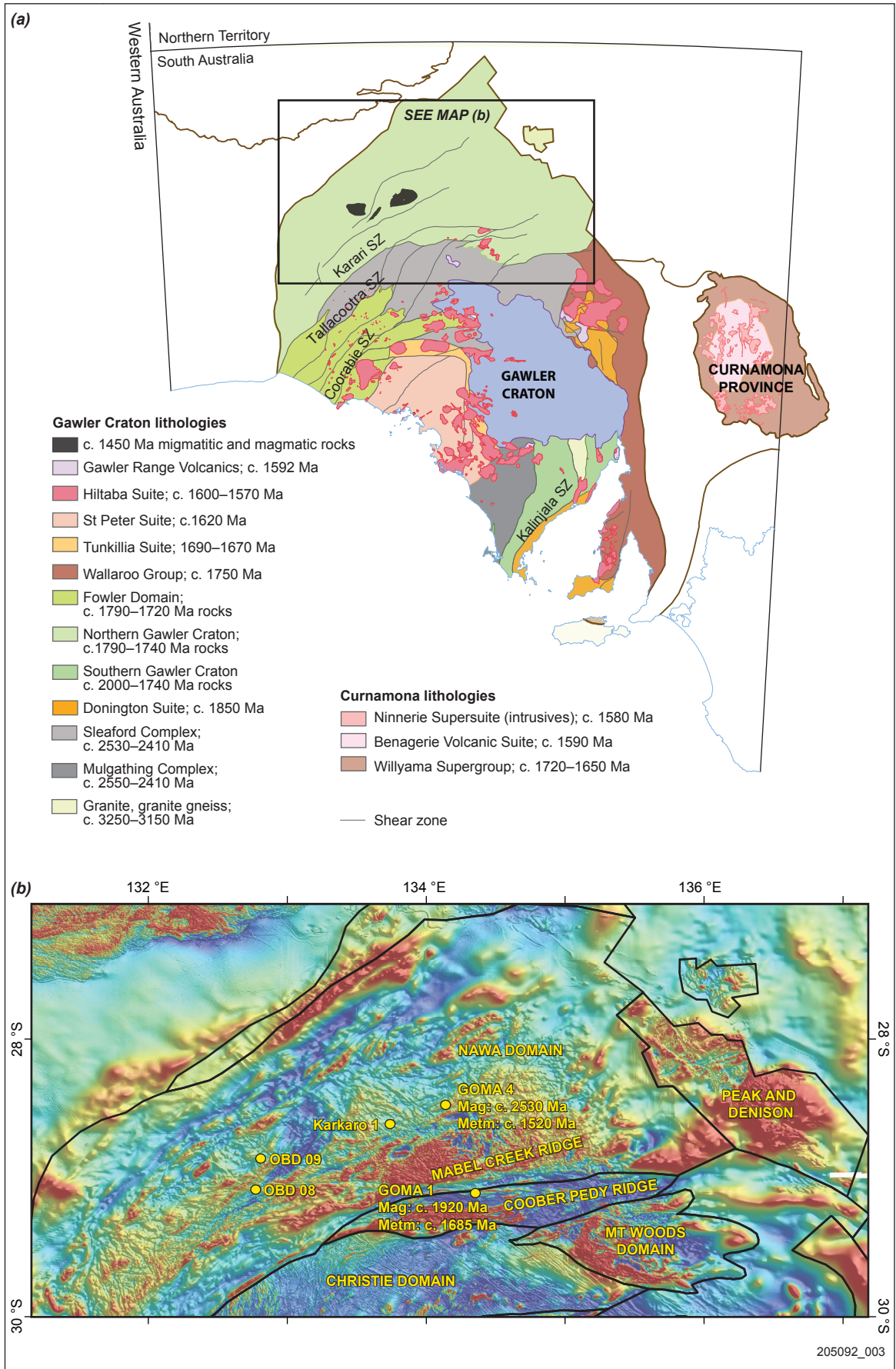


Figure 1 (a) Interpreted simplified solid geology map of the Gawler Craton, after Reid et al. (2014). (b) Total magnetic intensity reduced-to-pole image of the northern Gawler Craton, showing major geophysically defined domains. Geochronological data from drillholes of interest are from Reid et al. (2014). Reprinted from Morrissey et al. (2018; fig. 1) without locality map.

Table 1 Sample locations and summary

Drillhole	SA Geodata drillhole number	Easting*	Northing*	SA Geodata sample number	Sample interval (m)	Age (Ma) [†]	Lithology
OBD 09	1592	293375	6809107	1643403	389.30–389.80	—	Migmatitic garnet–cordierite–biotite gneiss
				2163654A	390.27–390.38	—	Migmatitic garnet–cordierite–biotite gneiss
				2163654B	390.38–390.47	—	Garnet–cordierite-bearing leucosome
				660842	391.95–392.25	—	Migmatitic garnet–biotite gneiss
				2163655	400.31–400.41	—	Migmatitic garnet–biotite gneiss
OBD 08	1577	286298	6788087	1643401	180.00–180.40	1444 ± 10 (monazite)	Migmatitic garnet–biotite gneiss
				2131380	183.00–184.00	1458 ± 9 (monazite)	Granite
						1463 ± 15 (zircon)	Granite
Karkaro 1	3552	380270	6835938	637614	477.39–477.57	1442 ± 9 (monazite)	Fine-grained granite
				637615	479.70–480.01	1463 ± 8 (monazite)	Coarse-grained granite

* GDA94, zone 53; † LA-ICP-MS U–Pb.

garnet–biotite-bearing gneiss that displays evidence for partial melting (Figs 2a–d). Two drillholes (OBD 08 and Karkaro 1) intersected unfoliated granite (Figs 2e–f). Samples from OBD 09 were used for metamorphic modelling and monazite geochronology to constrain the conditions and timing of metamorphism. Samples from OBD 08 and Karkaro 1 were used for monazite and zircon geochronology and geochemistry to determine the age and character of magmatism.

Analytical methods

Whole-rock chemical compositions of two samples of migmatitic gneiss from OBD 09 were obtained by X-ray fluorescence at Franklin and Marshall College, Pennsylvania. Phase equilibria models were calculated using THERMOCALC v3.40, using the internally consistent dataset, ds62, of Holland and Powell (2011) and activity–composition models re-parameterised for metapelitic rocks in the system MnNCKFMASHTO (MnO–Na₂O–CaO–K₂O–FeO–MgO–Al₂O₃–SiO₂–H₂O–TiO₂–Fe₂O₃) (Powell et al. 2014; White et al. 2014; White, Powell and Johnson 2014). Whole-rock geochemical compositions of magmatic rocks from OBD 08 and Karkaro 1 were obtained from Amdel Limited, South Australia. U–Pb zircon and monazite geochronology was done by laser ablation - inductively coupled plasma - mass spectroscopy (LA-ICP-MS) at Adelaide Microscopy, the University of Adelaide.

Pressure–temperature conditions and timing of metamorphism

The gneissic basement rocks intersected in OBD 09 contain garnet, biotite, plagioclase, K-feldspar, quartz, minor pyrite and amorphous magnesium-rich clay interpreted to reflect the former presence

of cordierite. They display a gneissic foliation defined by alternating biotite- and K-feldspar-rich layers. Leucosomes that are semi-concordant to discordant to the foliation are bounded by biotite–garnet melanosomes up to 1 cm in width (Figs 2a–c). Some of the leucosomes contain garnet and/or pseudomorphed cordierite. Therefore, the peak assemblages are interpreted to have developed in the presence of melt.

Pressure–temperature pseudosections for two samples from OBD 09 were calculated using the phase equilibria modelling program THERMOCALC. These suggest that peak conditions involved temperatures of 775–815 °C and pressures of 3.2–5.4 kbar (Fig. 3), corresponding to high apparent thermal gradients of >45 °C/km. The high apparent thermal gradients may reflect pluton-enhanced metamorphism, consistent with the presence of coeval A-type granites in drillholes OBD 08 and Karkaro 1. A sample of garnet-bearing migmatitic gneiss from drillhole OBD 09 gives a monazite age of 1444 ± 10 Ma (Fig. 4a), interpreted to date the timing of granulite facies metamorphism.

Age and character of magmatism

The granite in OBD 08 is medium-grained and contains K-feldspar, plagioclase, quartz and minor biotite. The K-feldspar is unaltered, but the plagioclase has been altered and hematite stained (Fig. 2e). Karkaro 1 intersects granite with coarse- and fine-grained phases (Fig. 2f). The two phases are mineralogically identical and contain K-feldspar phenocrysts, plagioclase, quartz and minor biotite that are aligned in what appears to be a magmatic flow foliation. As in OBD 08, plagioclase has been altered. Granitic rocks in both drillholes are undeformed.

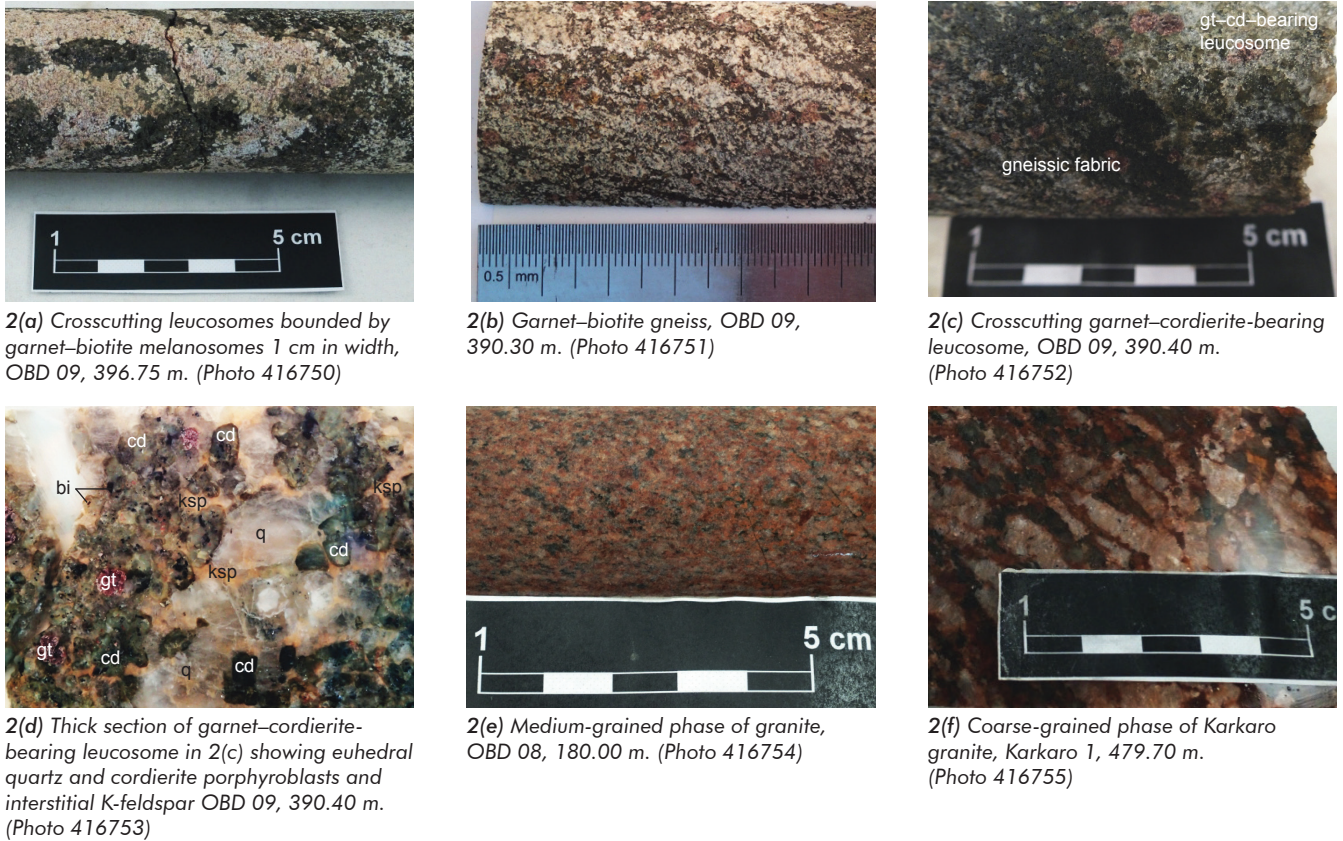


Figure 2 Photographs of lithologies from core yielding c. 1450 Ma ages. Reprinted from Morrissey et al. (2018; fig. 2).

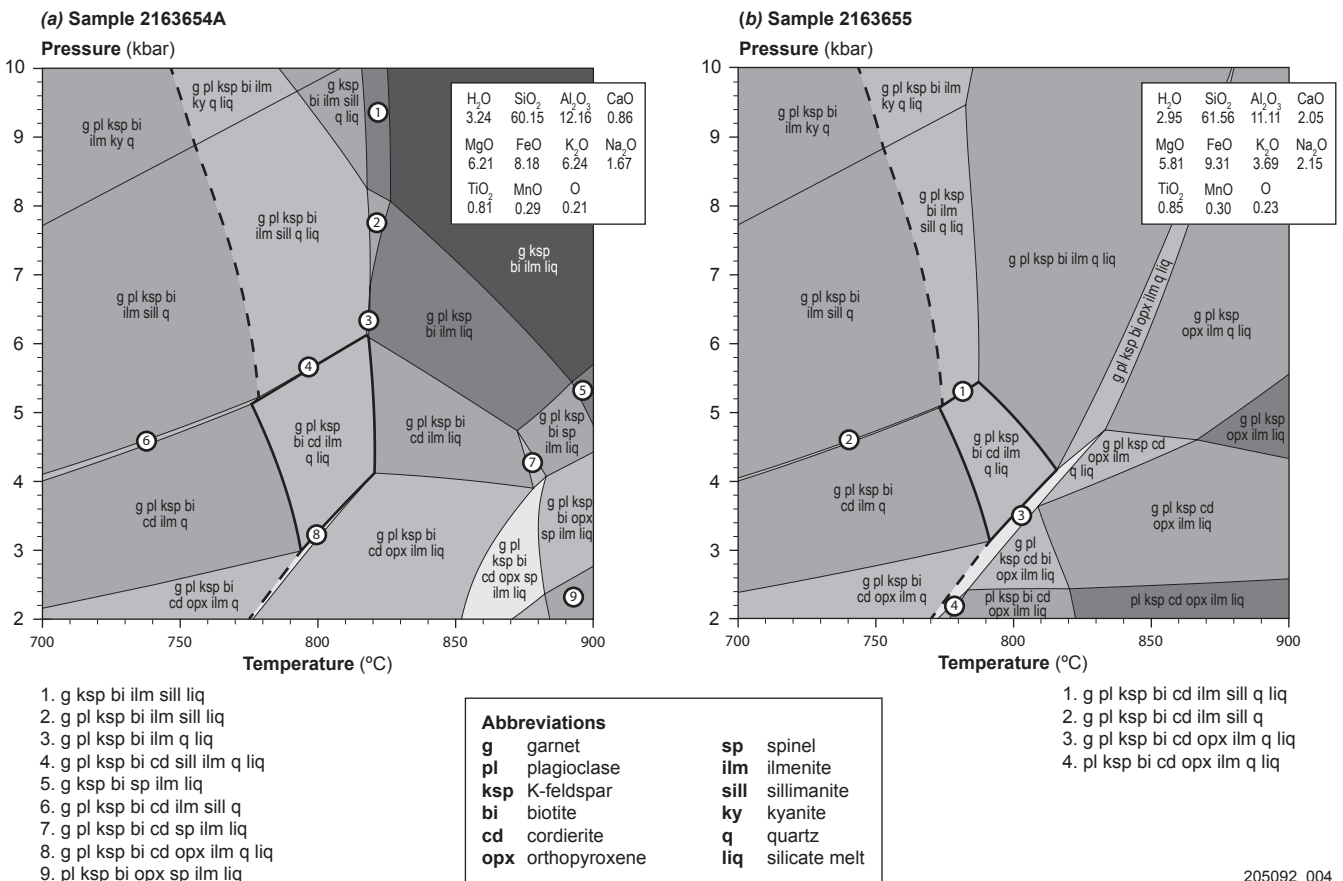
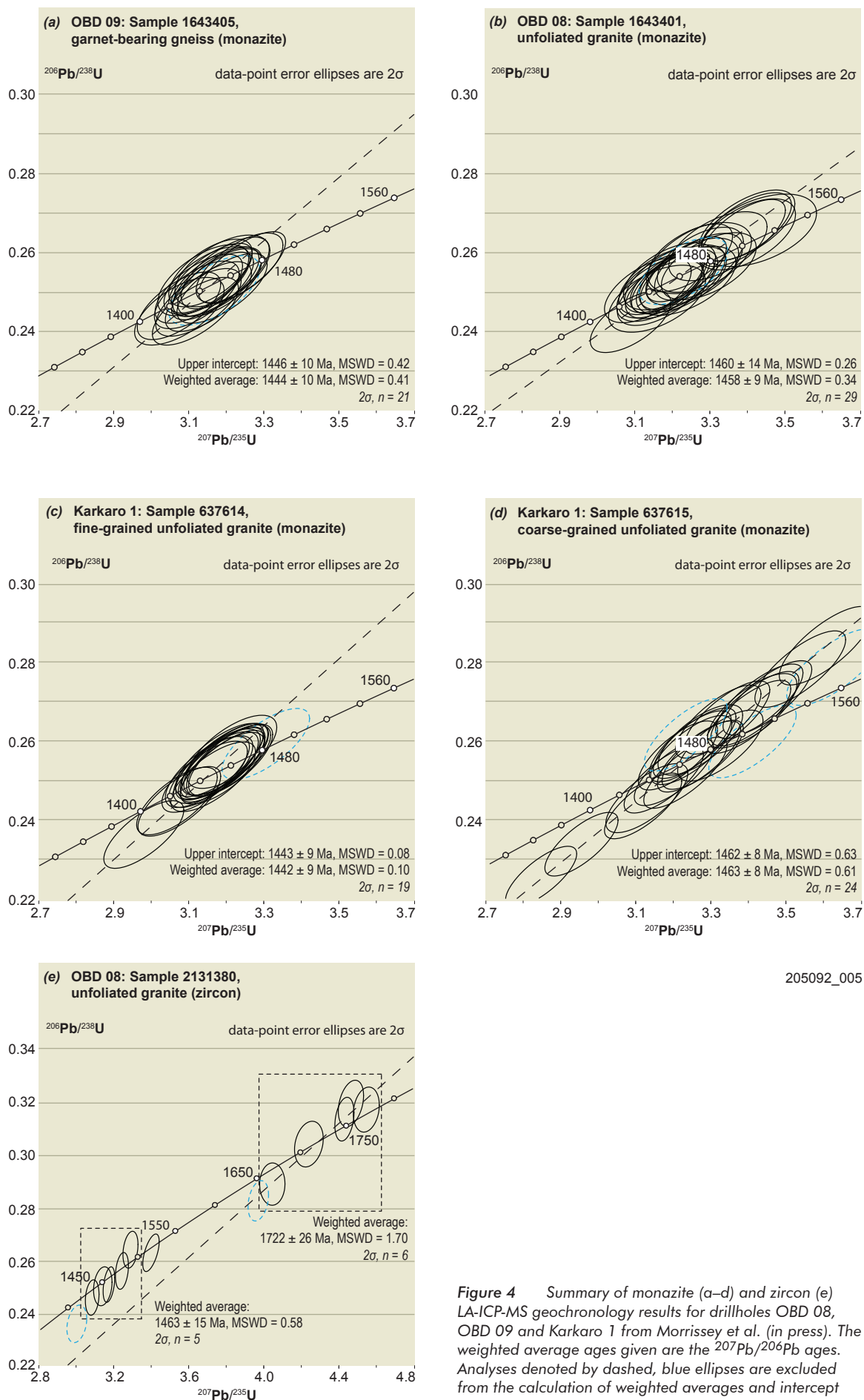


Figure 3 Calculated pressure–temperature pseudosections for two samples of garnet-bearing gneiss from drillhole OBD 09. The bulk rock composition in mol% is given in the box insets. The bold dashed line is the solidus. The interpreted peak field for each sample is outlined in bold. Reprinted from Morrissey et al. (2018; fig. 7).

205092_004



205092_005

Figure 4 Summary of monazite (a–d) and zircon (e) LA-ICP-MS geochronology results for drillholes OBD 08, OBD 09 and Karkaro 1 from Morrissey et al. (in press). The weighted average ages given are the $^{207}\text{Pb}/^{206}\text{Pb}$ ages. Analyses denoted by dashed, blue ellipses are excluded from the calculation of weighted averages and intercept ages. Reprinted from Morrissey et al. (2018; fig. 4).

LA-ICP-MS U–Pb monazite geochronology was collected from two samples from Karkaro 1 and one sample from OBD 08. The three samples give U–Pb monazite ages between 1463 ± 8 Ma and 1442 ± 9 Ma (Fig. 4b–d). Zircon geochronology was only possible from OBD 08, as the zircon grains from the Karkaro 1 samples were metamict and could not be analysed to provide meaningful age data. The zircon ages from OBD 08 come from bright, weakly zoned cores and define two populations at 1722 ± 26 Ma and 1463 ± 15 Ma (Fig. 4e). The oldest ages are consistent with the c. 1730–1690 Ma Kimban Orogeny, which affected much of the northern Gawler Craton (e.g. Payne et al. 2008). Therefore, the older ages are interpreted to be inherited from the source region or to have been entrained during melt emplacement. The younger (1463 ± 15 Ma) zircon age population is within uncertainty of the monazite age of 1458 ± 9 Ma for the same granite. Therefore, it is likely that the c. 1450 Ma monazite ages in each of the granitic samples reflects the timing of crystallisation of the granites.

Geochemistry and Sm–Nd isotope data from Morrissey et al. (in press) show these granites have high K_2O of 6.3–7 wt%, steep light rare earth element patterns, high Ga/Al values and initial ϵNd values of –14 to –8.7 (Fig. 5). These data suggest the granites are ‘A-type’ (Whalen, Currie and Chappell 1987) and derived predominantly from the melting of Archean crust.

Implications for the Gawler Craton

It is difficult to determine the wider spatial footprint and tectonic setting of 1450 Ma metamorphism due to the limited number of drillholes that intersect basement. One possible interpretation of this newly documented c. 1460–1440 Ma metamorphic event in the northern Gawler Craton is that it was driven by magmatism and is therefore relatively spatially localised. However, the drillholes containing c. 1460–1440 Ma magmatic and metamorphic rocks encompass a region of approximately 1,000 km² (Fig. 1; Table 1), and the presence of crustally derived, A-type magmatism in drillholes OBD 08 and Karkaro 1 indicates a larger region of elevated temperatures in the lower crust. Furthermore, ⁴⁰Ar/³⁹Ar thermochronological data (Fraser, Reid and Stern 2012) and apatite U–Pb data (Hall et al. 2018) from throughout the Nawa Domain indicate a broader thermal event at this time. A possible tectonic scenario that could produce distributed elevated heat flow is regional extension.

Elsewhere in the Gawler Craton, there is evidence for a possible extensional regime at c. 1500–1400 Ma, most notably with deposition of the Pandurra Formation in the Cariewerloo Basin (Beyer et al. 2018). The Pandurra Formation is interpreted to have been deposited in half grabens in fluvial and lacustrine paleoenvironments as part of a continental rift system after c. 1490 Ma (Beyer et

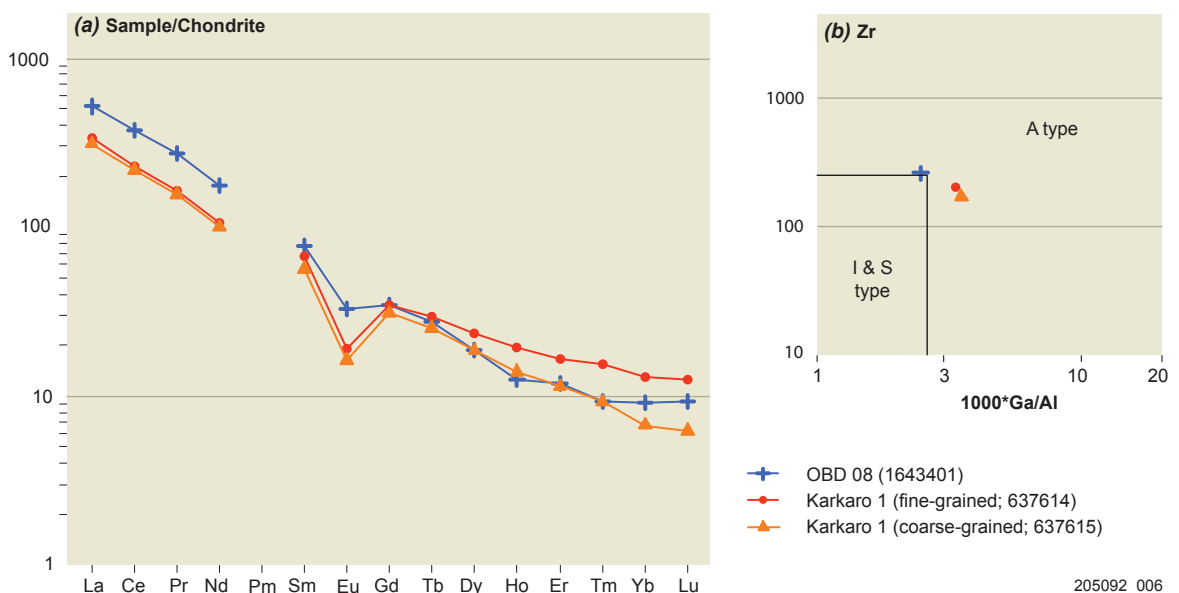


Figure 5 Geochemical plots for magmatic samples, OBD 08 and Karkaro 1. (a) Rare earth elements chondrite spider plot after Boynton (1984). (b) Zr–Ga/Al plot after Whalen, Currie and Chappell (1987). Reprinted from Morrissey et al. (2018; figs 5c, d).

al. 2018). After deposition, fluid flow events in the Pandurra Formation occurred at c. 1450–1420 Ma (Cherry et al. 2017; Beyer et al. 2018). Lithospheric-scale shear zones in the Gawler Craton, including the Karari, Tallacootra, Coorabie and Kalinjala shear zones (Fig. 1a), were active or were re-activated between 1470–1450 Ma (Foster and Ehlers 1998; Swain et al. 2005; Fraser and Lyons 2006; Thomas, Direen and Hand 2008; Fraser, Reid and Stern 2012), confirming the presence of regional deformation in this interval. Therefore, it is possible that the high temperatures in the Nawa Domain, reactivation of crustal-scale shear zones across the craton and the formation of a significant, intracontinental sedimentary basin in the central-eastern Gawler Craton are all part of a coherent tectonic regime dominated by extension.

Implications for Mesoproterozoic mineral potential or fluid flow events

The mineral potential associated with the widespread record of c. 1450 Ma deformation, metamorphism, magmatism and sedimentation across the Gawler Craton remains uncertain. There is no known mineralisation within the northern Gawler Craton, which was the region most significantly affected by this Mesoproterozoic thermal event. Nevertheless, the presence of high-crustal level granites in some portions of the northern Gawler Craton may suggest the potential for mineralisation related to these intrusions, or possibly related to fluid flow driven by the combination of deformation, magmatism and associated sedimentary basin formation in an overall extensional environment. The redbed successions of the Carriewerloo Basin could have provided a source of fluid that interacted with basement in the central and eastern Gawler Craton. Indeed, recent evidence for clasts of sandstone correlated with the Pandurra Formation occurring within the Olympic Dam Breccia Complex suggests that this sedimentary basin did interact with the basement rocks (Cherry et al. 2017). The timing of the second phase of deformation and fluid flow that incorporated the Pandurra Formation sandstone into the Olympic Dam Breccia Complex is uncertain (Cherry et al. 2017), but it may plausibly correlate to the c. 1460–1440 Ma event. Hence, there is potential that fluid flow could have occurred within the basement across the Gawler Craton, especially within shear zones related to the development of the Carriewerloo Basin. Shear zones are therefore targets for mineral exploration as potential conduits of high temperature fluids related to the c. 1450 Ma event.

Acknowledgements

The staff at Adelaide Microscopy are thanked for technical assistance and the staff at the South Australia Drill Core Reference Library are thanked for assistance with sampling. This project was supported by ARC Linkage Project LP160100578 (J Payne and M Hand) and ARC Discovery Project DP160104637 (M Hand).

References

- Beyer SR, Kyser K, Polito PA and Fraser GL 2018. Mesoproterozoic rift sedimentation, fluid events and uranium prospectivity in the Carriewerloo Basin, Gawler Craton, South Australia. *Australian Journal of Earth Sciences* 65:409–426.
- Boynton 1984. Cosmochemistry of the rare earth elements: meteorite studies. *Developments in Geochemistry* 2, 63e114.
- Cherry AR, McPhie J, Kamenetsky VS, Ehrig K, Keeling JL, Kamenetsky MB, Meffre S and Apukhtina OB 2017. Linking Olympic Dam and the Carriewerloo Basin: was a sedimentary basin involved in formation of the world's largest uranium deposit? *Precambrian Research* 300:168–180.
- Cutts K, Hand M and Kelsey DE 2011. Evidence for early Mesoproterozoic (ca. 1590Ma) ultrahigh-temperature metamorphism in southern Australia. *Lithos* 124:1–16.
- Fairclough M, Schwarz M and Ferris GM 2003. *Interpreted crystalline basement geology of the Gawler Craton, South Australia 1:1,000,000 Special Map, Plan 201853. Primary Industries and Resources South Australia, Adelaide.*
- Foster DA and Ehlers K 1998. ^{40}Ar - ^{39}Ar thermochronology of the southern Gawler Craton, Australia: implications for Mesoproterozoic and Neoproterozoic tectonics of East Gondwana and Rodinia. *Journal of Geophysical Research* 103:10177–10193.
- Fraser GL and Lyons P 2006. Timing of Mesoproterozoic tectonic activity in the northwestern Gawler Craton constrained by $^{40}\text{Ar}/^{39}\text{Ar}$ geochronology. *Precambrian Research* 151:160–184.
- Fraser G, Reid A and Stern R 2012. Timing of deformation and exhumation across the Karari Shear Zone, northwestern Gawler Craton, South Australia. *Australian Journal of Earth Sciences* 59:547–570.
- Hall JW, Glorie S, Reid AJ, Boone SC, Collins AS and Gleadow A 2018. An apatite U–Pb thermal history map for the northern Gawler Craton, South Australia. *Geoscience Frontiers* 9:1293–1308.
- Holland TJB and Powell R 2011. An improved and extended internally consistent thermodynamic dataset for phases of petrological interest, involving a new equation of state for solids. *Journal of Metamorphic Geology* 29:333–383.
- Howard KE, Hand M, Barovich KM, Payne JL, Cutts KA and Belousova EA 2011. U–Pb zircon, zircon Hf and whole-rock Sm–Nd isotopic constraints on the evolution of Paleoproterozoic rocks in the northern Gawler Craton. *Australian Journal of Earth Sciences* 58:615–638.

- Morrissey LJ, Barovich KM, Hand M, Howard KE and Payne JL in press. Magmatism and metamorphism at ca. 1.45 Ga in the northern Gawler Craton: the Australian record of rifting within Nuna (Columbia). *Geoscience Frontiers* (2018).
- Payne JL, Barovich K and Hand M 2006. Provenance of metasedimentary rocks in the northern Gawler Craton, Australia: implications for Palaeoproterozoic reconstructions. *Precambrian Research* 148:275–291.
- Payne JL, Hand M, Barovich KM and Wade BP 2008. Temporal constraints on the timing of high-grade metamorphism in the northern Gawler Craton: implications for assembly of the Australian Proterozoic. *Australian Journal of Earth Sciences* 55:623–640.
- Payne J, Raimondo T, Morrissey L, Hand M, Lilly R, Tomkins A, Reid A, Dutch R, Wade C, Hamisi J, Bockmann M and Janicki M 2018. Source to Spectrum: project update. *MESA Journal* 88:12–14. Department for Energy and Mining, Adelaide.
- Powell R, White RW, Green ECR, Holland TJB and Diener JFA 2014. On parameterizing thermodynamic descriptions of minerals for petrological calculations. *Journal of Metamorphic Geology* 32:245–260.
- Reid AJ, Jagodzinski EA, Armit RJ, Dutch RA, Kirkland CL, Betts PG and Schaefer BF 2014. U-Pb and Hf isotopic evidence for Neoproterozoic and Paleoproterozoic basement in the buried northern Gawler Craton, South Australia. *Precambrian Research* 250:127–142.
- Swain GM, Hand M, Teasdale J, Rutherford L and Clark C 2005. Age constraints on terrane-scale shear zones in the Gawler Craton, southern Australia. *Precambrian Research* 139:164–180.
- Thomas JL, Direen NG and Hand M 2008. Blind orogen: integrated appraisal of multiple episodes of Mesoproterozoic deformation and reworking in the Fowler Domain, western Gawler Craton, Australia. *Precambrian Research* 166:263–282.
- Whalen JB, Currie KL and Chappell BW 1987. A-type granites: geochemical characteristics, discrimination and petrogenesis. *Contributions to Mineralogy and Petrology* 95:407–419.
- White RW, Powell R, Holland TJB, Johnson TE and Green ECR 2014. New mineral activity–composition relations for thermodynamic calculations in metapelitic systems. *Journal of Metamorphic Geology* 32:261–286.
- White RW, Powell R and Johnson TE 2014. The effect of Mn on mineral stability in metapelites revisited: new α - x relations for manganese-bearing minerals. *Journal of Metamorphic Geology* 32:809–828.

FURTHER INFORMATION

Laura Morrissey
Laura.Morrissey@unisa.edu.au

Source to Spectrum: project update

Justin Payne^{1, 2}, Tom Raimondo^{1, 2}, Laura Morrissey^{1, 2}, Martin Hand², Richard Lilly², Andrew Tomkins³, Anthony Reid⁴, Rian Dutch⁴, Claire Wade^{4, 2}, Jonathan Hamisi³, Mitchell Bockmann² and Matthew Janicki¹

¹ School of Natural and Built Environments, University of South Australia

² School of Physical Sciences, University of Adelaide

³ School of Earth, Atmosphere and Environment, Monash University ⁴ Geological Survey of South Australia, Department for Energy and Mining

Introduction

The Source to Spectrum project (S2S) is focused on understanding the formation and likelihood of preservation of the spectrum of base and precious metal deposits associated with the c. 1595–1570 Ma Hiltaba Suite and Gawler Range Volcanics magmatic event (Payne et al. 2017). This sees us shifting the focus of research away from the extensively discussed and researched Olympic iron oxide – copper–gold (IOCG) province to the regions of the Gawler Craton that have received less attention in the past decade. This article provides a brief overview of the research that is currently being undertaken, initial results from a number of studies and upcoming outputs from the project.

The right time and place

One module of the S2S project is focused on constraining the age of alteration and mineralisation, and the age of the host lithologies and their metamorphic history. To date this work has focused on the Mount Woods Domain, southern Gawler Range Volcanics region, and Central Gawler Gold Province. Some of the key findings to date are:

- A Wallaroo Group equivalent metasedimentary host has been determined for the Barns gold prospect that was metamorphosed during the Kimban Orogeny. This adds to the range of host lithologies for gold mineralisation, already including the Tarcoola Formation, Tunkillia Suite granites and Archean gneisses, and further demonstrates that the host lithology and metamorphic grade is not a primary control on deposit formation.
- Host volcanics of the Paris silver deposit are confirmed as lower Gawler Range Volcanics (1592 Ma; Fig. 1). Attempts to constrain the age of a second rhyolite dyke that is related to mineralisation have not been successful so far.

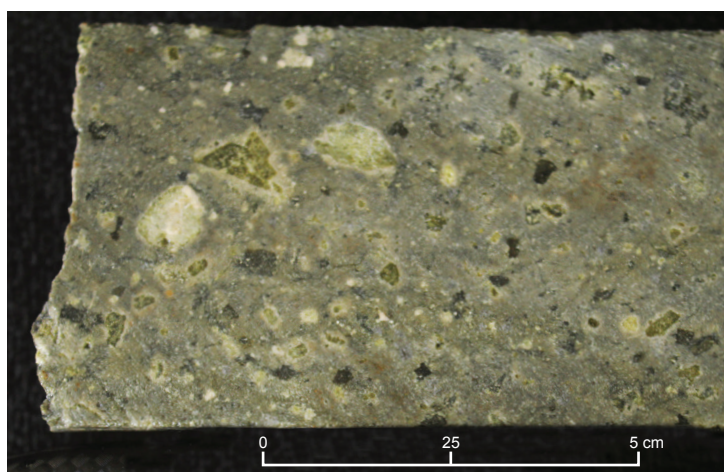


Figure 1 Lower Gawler Range Volcanics, host to the Paris silver deposit, drillhole PPDH001, 111.93–113.85 m. (Courtesy of Investigator Resources; photo 416756)

- Granulite facies metamorphism within the central and eastern Mount Woods Domain is dominantly Kimban Orogeny aged (Fig. 2). This provides renewed potential for preservation of upper crustal c. 1590 Ma mineral deposits in these regions, as opposed to exhumation of mid-to-lower crustal c. 1590 Ma granulite facies rocks which would have resulted in the erosion of any mineral deposits. Preliminary interpretations suggest c. 1590 Ma metamorphism and recrystallisation is dominantly related to discrete shear zone movement, intrusions and/or alteration systems. Monazite from a garnet-bearing granitic gneiss preserves a Sleafordian Orogeny crystallisation age, providing the first evidence for Archean – early Paleoproterozoic crust in the Mount Woods Domain (Janicki 2018).
- A-type magmatism and high thermal gradient metamorphism in the Karkaroo and OBD series drillholes in the Nawa Domain are constrained to c. 1450 Ma (Morrissey et al. in press).

Development of titanite U–Pb laser ablation - inductively coupled plasma - mass spectroscopy (LA-ICP-MS) geochronology in South Australia as

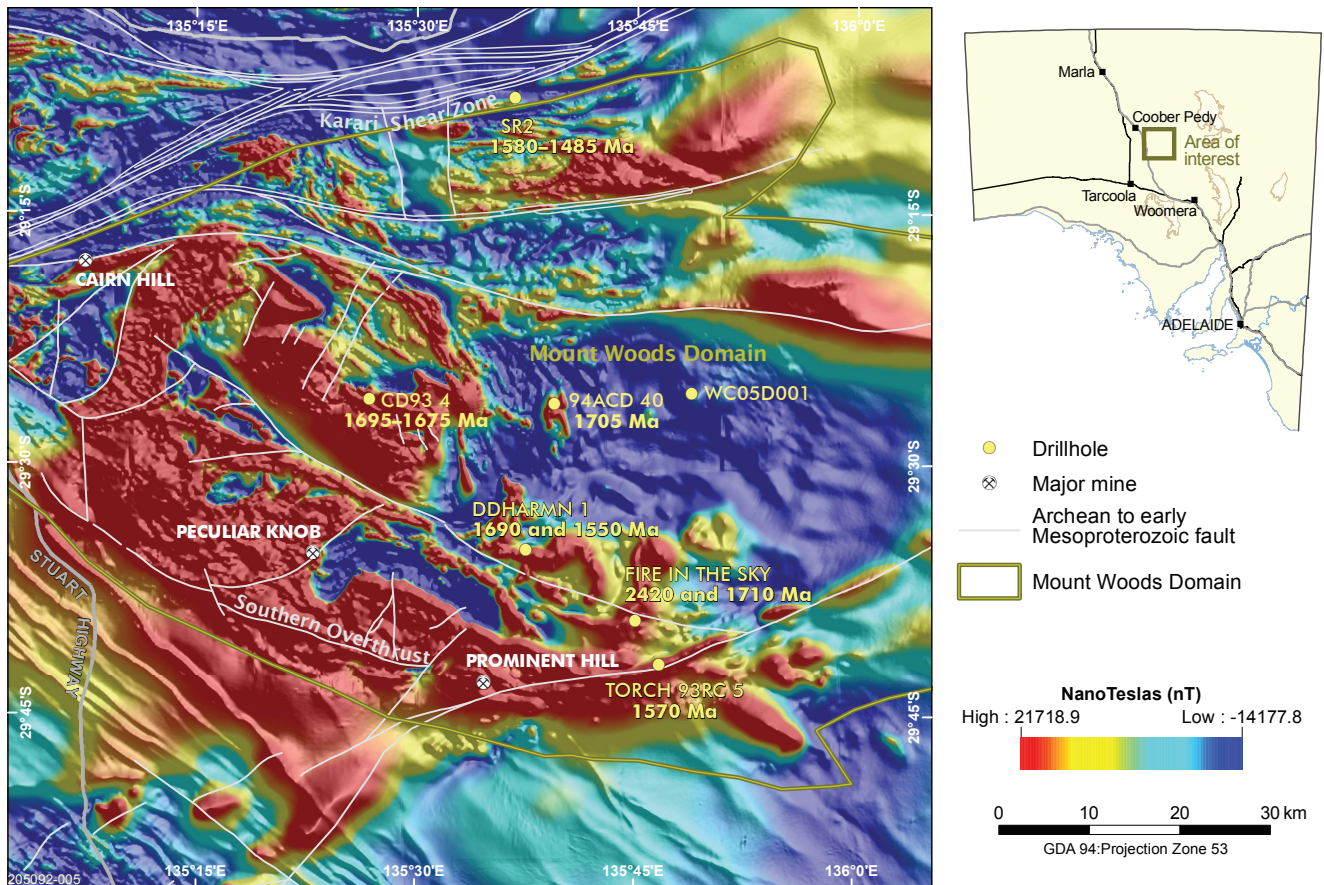


Figure 2 Total magnetic intensity reduced-to-pole image of the Mount Woods Domain with sampled drillholes and representative U–Pb monazite geochronology ages. Ages provided are rounded to nearest 5 Ma to provide an indicator of the age ranges present.

part of S2S means we are now able to rapidly determine the age of titanite-bearing alteration and mineralisation systems. The first application of this method is to a range of skarn Cu–Au/Au and iron sulfide – copper–gold mineralisation systems, with results to be presented at the [Geological Survey of South Australia Discovery Day 2018](#). We are also interested in knowing of any drillholes in the Gawler Craton that contain titanite formed during alteration and mineralisation. To this extent we would be pleased to hear from any geologists who know of such drillholes.

Research efforts in the coming year will focus on obtaining precise age constraints on gold, silver and base metal deposits to determine if they can be directly linked to certain phases of activity within the Gawler Range Volcanics and Hiltaba Suite.

Metal and fluid sources

Studies are in progress at Monash University and the University of South Australia looking at the generation and character of fluids in the full spectrum of mineralising systems in the Gawler Craton. Phase equilibria modelling and

experimental work is focused on determining the role of minerals such as scapolite in the generation of halogen and sulfur-rich fluids in the mid-crust during metamorphism (regional or contact) as a non-magmatic source of fluids. This will be used to assess the importance of basin-fill sequences in the generation of mineral deposits such as IOCGs.

The Central Gawler Gold Province has previously been the focus of research but those studies were unable to conclusively determine if the gold deposits were driven by metamorphic or magmatic processes. S2S is reassessing this issue by investigating deposits with a wider variety of host lithologies and undertaking an in-depth study of the mafic and volcanic dykes that are near ubiquitous in the deposits.

Ongoing research on the broader Hiltaba Suite intrusives is investigating the spatial variation in the composition of their crust and mantle components. Preliminary results highlight the widespread presence of an anomalously enriched or contaminated mantle reservoir. We are yet to determine the importance of this compositional reservoir for mineral deposit formation.

Complementing the Central Gawler Gold Province and magmatic geochemistry study is a stable isotope and trace element geochemistry investigation into the deposits and prospects distributed across the southern Gawler Range Volcanics province. Initial results indicate that Barns gold and Paris silver are consistent with a magmatic petrogenesis (Morrissey et al. 2017). Skarn-style deposits have variable crustal input with a recycled Archean component present in the Weednanna Au–Fe skarn.

References

- Janicki M 2018. Constraining areas of possible prospectivity in the Mt Woods region of the Gawler Craton using geochronological methods. Hons thesis, University of South Australia, Adelaide.
- Morrissey LJ, Barovich KM, Hand M, Howard KE and Payne JL in press. Magmatism and metamorphism at ca. 1.45 Ga in the northern Gawler Craton: the Australian record of rifting within Nuna (Columbia). *Geoscience Frontiers* (2018).
- Morrissey L, LaFlamme C, Payne J and Raimondo T 2017. S isotopes across the Gawler Craton: new data on ore sources. *Geological Survey of South Australia Discovery Day 2017: presentation abstracts and posters, Report Book 2017/00036*. Department of the Premier and Cabinet, South Australia, Adelaide, pp. 50–51.
- Payne J, Raimondo T, Morrissey L, Hand M, Lilly R, Tomkins A, Reid A, Dutch R and Wade C 2017. Source to Spectrum: a new project investigating the range of mineral deposits in the Gawler Craton. *MESA Journal* 83:8–10. Department of the Premier and Cabinet, South Australia, Adelaide.

FURTHER INFORMATION

Justin Payne
Justin.Payne@unisa.edu.au

Spectral analysis of drill core from the Kanmantoo copper deposit

Alan Mauger¹, John Keeling¹, Peter Rolley² and Hayden Arbon²

¹ Geological Survey of South Australia, Department for Energy and Mining

² Hillgrove Resources

Introduction

The Kanmantoo copper deposit describes a cluster of eight zones of Cu–Ag–Au mineralisation located ~2.5 km southwest of Kanmantoo township, 41 km southeast of Adelaide. Hydrothermal chalcopyrite–pyrite–pyrrhotite–magnetite mineralisation is concentrated in structurally controlled zones within biotite, quartz, andalusite, chlorite, garnet ± staurolite schist within the western limb of the Kanmantoo syncline. Copper production began in the late 1840s with underground mining of small high-grade lodes, followed by open pit mining in 1970–76 (Verwoerd and Cleghorn 1975) and most recently in 2011 to present, with expanded open pit operations by Hillgrove Resources. Past production and current resource estimates give a metal endowment at Kanmantoo of around 0.35 Mt of copper, 3 Moz of silver and 100 koz of gold (Rolley and Wright 2017). Estimated remaining total mineral resources, as at 31 December 2017, were 31.8 Mt at 0.6% Cu, 0.1 g/t Au, 1.3 g/t Ag, for cutoff grade 0.2% Cu (Hillgrove Resources 2018).

Continuous spectral analysis of selected drill core from various mineralised zones at Kanmantoo was completed recently by the Geological Survey of South Australia in collaboration with Hillgrove Resources to map mineralogy and mineral associations. The results have been used to assist with interpreting proximity to mineralisation. This article provides an overview of the project and findings. The approach may be useful in assessing the potential for further mineralisation within known ore systems at Kanmantoo and offers a means of acquiring high data density for evaluating patterns of hydrothermal activity identified in exploration drill samples from other copper targets in the district.

Geological setting and mineralisation

Copper mineralisation at Kanmantoo is hosted by the Tapanappa Formation within the Cambrian Kanmantoo Group, a 7–8 km thick package of dominantly marine turbidite sediments deposited in an extensional back-arc basin, the Kanmantoo Trough (Haines, Jago and Gum 2001). The sedimentary pile was accumulated over a comparatively short 8 ± 5 Ma period between 522 ± 2 to 514 ± 3 Ma (Foden et al. 2006). The Tapanappa Formation consists of a largely monotonous sequence of immature sandstone (greywacke) with muddy siltstone interbeds and minor pyritic mudstone (Toteff 1999). In addition to the Kanmantoo deposit, the sequence hosts several smaller deposits of Cu–Au mineralisation (e.g. Bremer, South Hill) and scattered occurrences and deposits of Pb–Zn–Ag, some of which have been mined (e.g. Angas, Wheal Ellen, Aclare, Strathalbyn, Scotts Creek) (Belperio et al. 1998; Both 1990; Gum 1998; Seccombe et al. 1985; Spry, Schiller and Ross 1988; Toteff 1999). Much of the Pb–Zn–Ag mineralisation is stratabound and coincident with sites of apparent alteration of the sediment, expressed as zones of quartz–biotite–garnet–andalusite ± staurolite rock that can be traced intermittently for ~30 km from north of Kanmantoo, south towards Strathalbyn (Fig. 1) (Seccombe et al. 1985; Toteff 1999; Pollock et al. 2018). The garnetiferous rocks are broadly anomalous in Pb, Zn, Cu and Mn (Pollock et al. 2018). The pattern of alteration and distribution of mineralisation, particularly Pb–Zn–Ag, in the Tapanappa Formation are interpreted as evidence of synsedimentary hydrothermal exhalative activity with metals deposited from heated basin fluids channelled along growth faults accompanying extension of the basin (Flöttmann et al. 1984; Seccombe et al. 1985; Toteff 1999).

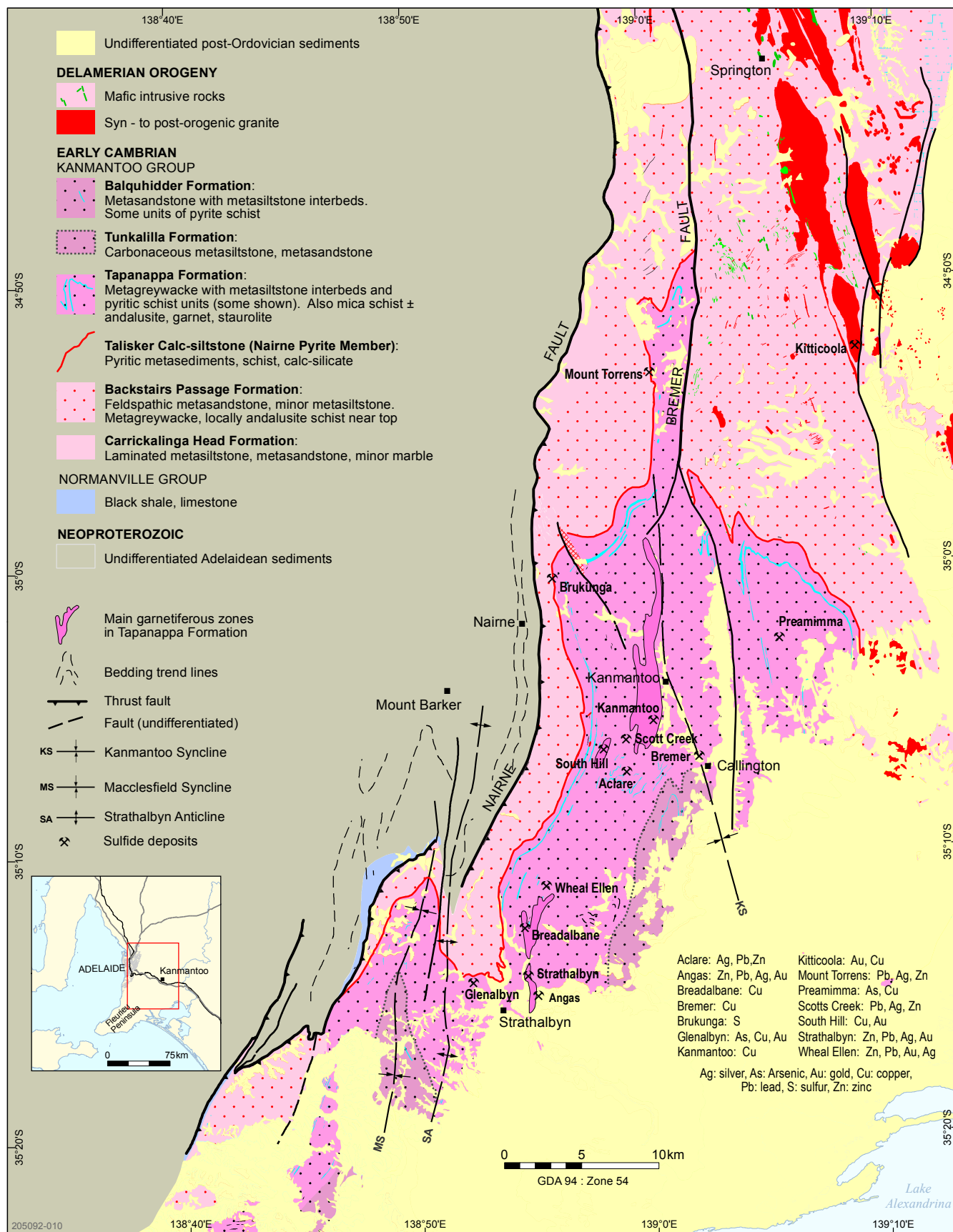


Figure 1 Geology of the Kanmantoo region showing the location of Kanmantoo Cu–Au deposit and regional Pb–Zn–Ag (Cu–Au) and Cu–Au deposits (updated from Toteff 1999).

Sedimentation in the Kanmantoo Trough ceased with the onset of the Delamerian Orogeny during the mid-Cambrian (514 Ma). Compressive deformation was accompanied by emplacement of syntectonic I- and S-type granitoids along the eastern Kanmantoo Trough, with A-type granite and mafic and felsic dykes intruded during post-tectonic (490–480 Ma) relaxation and extension (Belperio et al. 1998; Foden et al. 2002). Three phases of deformation are recognised with D1 NW-directed thrusting imparting bedding parallel schistosity that was overprinted by axial plane crenulation cleavage developed during D2 upright open to tight folds with dominantly N–S axes and gentle southerly plunges (Offler and Fleming 1968). Kanmantoo Syncline is a D2 structure that includes an open synformal structure that plunges ~15°S. A parasitic syncline of the Kanmantoo Syncline occupies two-thirds of the main pit at the Kanmantoo mine (Rolley and Wright 2017; Schiller 2000). Later deformation, D3, developed open to tight folds about NW–SE axes, which are rarely evident at Kanmantoo where the D3 event is usually observed only as crenulations and kinks (Schiller 2000). Metamorphism was high temperature (550–600 °C), low pressure (3–5 kb) and reached amphibolite facies in the region of Kanmantoo with peak metamorphism possibly post D2, reflected in iron-rich garnet growth and recrystallisation of biotite in discordant zones that also contain chlorite and sulfides (Rolley and Wright 2017). This is in contrast with pre to early D2 peak metamorphism in the Karinya Syncline in Kanmantoo Group rocks some 80 km to the north of the mine area (Sandiford et al. 1995).

Mineralisation at Kanmantoo is discordant to bedding but is broadly aligned with D2 schistosity on the western synform limb (Schiller 2000). The discordance is explained in sedimentary exhalative models as a subsurface hydrothermal feeder zone with remobilisation of sulfides during metamorphism (Pollock et al. 2018; Spry, Schiller and Ross 1988; Toteff 1999). An alternative model favours emplacement of Cu–Ag–Au mineralisation post peak metamorphism with mineralising fluids introduced by igneous intrusion at depth and circulated along reactivated D2 and crosscutting NNE and NE structures; metal deposition resulted from interaction of fluids with reactive host rocks or a decrease in the thermal gradient (Arbon 2011; Lyons 2012; Oliver et al. 1998; Rolley and Wright 2017; Tedesco 2009).

Despite some lingering controversy with regard to the origin of the Cu–Au–Ag mineralisation at Kanmantoo, the data collected in previous and ongoing studies point to a role for spectral analysis and mineral mapping. In particular, attention was directed to:

- amphibolite-grade metamorphic minerals equated with possible zones of hydrothermally altered sediments (e.g. andalusite, garnet, staurolite, spinel)
- mineral alteration indicative of later hydrothermal fluid interactions (e.g. reduction in andalusite content, change in garnet or biotite composition, crystallisation and composition of chlorite, presence of carbonate or sulfate minerals)
- minerals most closely associated with copper mineralisation (chlorite–sulfides–magnetite).

The objective was to collect and analyse continuous spectral data of drill core to provide a mineralogical model that characterised alteration zoning around copper mineralisation at Kanmantoo, which could be used to assist in improving the effectiveness of subsequent brownfields drilling.

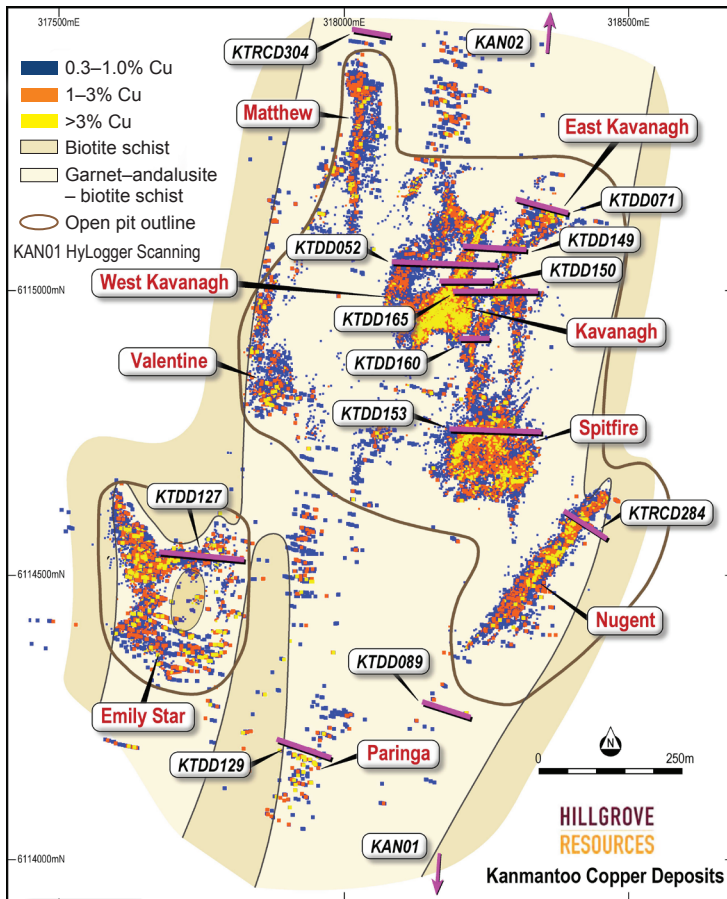
Spectral scanning and analysis

Continuous spectral data from drill core were collected using the HyLogger 3.3 instrument located at the South Australia Drill Core Reference Library at Tonsley. HyLogger 3.3 has a bank of four instruments – camera, visible-shortwave infrared (VSWIR; 400–2,500 nm) spectrometer, thermal infrared (TIR; 6,000–14,500 nm) spectrometer and a laser altimeter – under which core trays are moved on a robotic table. The collation of the data from these four instruments delivers an interactive digital file which enables the identification of a suite of minerals from a well characterised spectral library (Schodlock et al. 2016; Schodlock Green and Huntington 2016).

Fourteen legacy diamond drillholes were selected to encompass the breadth, lateral and vertical extent of the Kanmantoo copper mineralisation (Table 1; Fig. 2).

Based on previous investigations identifying key mineral components of the deposit that showed spectral responses in the shortwave infrared (SWIR) and TIR the following minerals were selected for more detailed analysis: kaolin/jarosite, white mica, andalusite, garnet (almandine), biotite and chlorite.

Variation in andalusite content was associated with persistent, but minor amounts, of kaolin and jarosite, not previously reported but evident in SWIR data recorded by HyLogger and quantified using the Spectral Assistant (TSA) software in the Spectral Geologist (TSG) software (Schodlock et al. 2016). The significance of kaolin/jarosite was further investigated using scanning electron microscopy (SEM) on selected samples from KTDD149. Fragments of drill core were mounted on aluminium stubs using araldite and coated with carbon. These were examined at Adelaide Microscopy on a FE Quanta 600 SEM with energy dispersive X-ray analytical facility.



205092_014

Figure 2 Distribution of copper across orebodies at Kanmantoo showing location of drillholes included in the initial spectral analysis investigation.

Table 1 Legacy drillholes selected for analysis from orebodies within the Kanmantoo copper deposit

Drillhole	SA Geodata drillhole number	Orebody or target
DDH KAN 2	206089	Distal North
KTRCD304	304265	Matthew
KTDD071	*	East Kavanagh
KTDD149	290347	East Kavanagh
KTDD150	*	Kavanagh
KTDD165	*	Kavanagh
KTDD052	*	West Kavanagh
KTDD160	290348	Kavanagh
KTDD153	*	Spitfire
KTRCD284	*	Nugent
KTDD089	*	Nugent
KTDD129	*	Paringa
KTDD127	*	Emily Star
DDH KAN 1	206088	Distal South

* Number will be assigned in first quarter 2019.

For white mica, the identification and relative abundance were calculated using TSA. Variation in the chemistry of the white mica was assessed based on the position of the wavelength minima for the 2,200 nm absorption feature.

Andalusite is a highly visible component in the core samples and forms white poikiloblastic porphyroblasts in biotite schist with varying degrees of coherence. The andalusite grains range from compact euhedral grains up to 2 cm in length overprinting the schistosity to somewhat diffuse masses, grading further to ghost outlines in the core.

Spectral absorption features for andalusite overlap with garnet. In order to map relative abundance of andalusite the TIR spectra were interpreted with the aid of polynomial fitting (PFIT). By focusing on the 10,365 nm absorption feature (Fig. 3) subtle contributions from andalusite were measured using the wavelength position. Andalusite abundance was calculated from the depth of the feature.

Garnet is a complex mineral with a wide range of chemical composition which may be present within a single grain, typically as concentric zones of varying composition. Major element compositions of garnet in the Kanmantoo deposit were measured by McPherson (2017) and results from the Kavanagh orebody are shown in Table 2. The analyses record garnet as dominantly almandine (Fe garnet), with lesser components of pyrope (Mg garnet) and spessartine (Mn garnet). The resolution of the HyLogger spectra (1 cm x 1 cm sample per spectra) means that the TIR spectra will be a composite of those individual species. This provides an opportunity to map geochemical gradients reflected in the change in overall garnet composition, determined by measuring wavelength shifts in the characteristic absorption features. To identify almandine, PFIT was used focusing on the wavelength of the 11,279 nm feature (Fig. 3) and the depth was used to estimate abundance. To measure changing chemistry, the wavelength of the 10,710 nm absorption feature was extracted. This was intended to map the proportion of Fe-garnet almandine (10,710 nm) relative to Mn-garnet spessartine (10,860 nm).

In hot hydrothermal systems, trioctahedral micas may be recrystallised with modified chemistry due to interaction with the hydrothermal fluid. At the Yangyang iron oxide – apatite deposit, South Korea, Kim et al. (2018) report hydrothermally altered biotite with modified SWIR spectral response, where the wavelengths of key absorption features were used to map change in visible colour and Fe:Mg ratio. The abundance of biotite at Kanmantoo offered the opportunity to investigate similar correlations in relation to copper mineralisation. To calculate an appropriate measure of geochemical

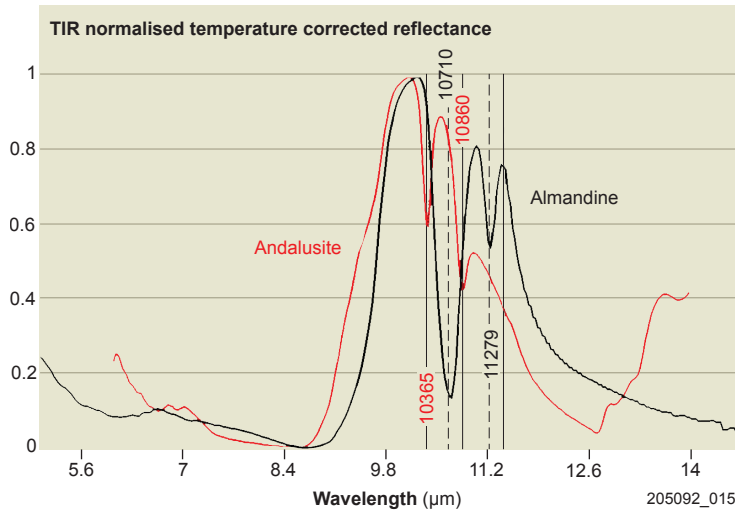


Figure 3 TIR spectra for andalusite and almandine showing the absorption features used to estimate occurrence and abundance.

Table 2 Average major element compositions for garnet from Kavanagh orebody (from McPherson 2017)

Sample number	54-2	54-3	54-4	54-9
Depth (m)	6.00	10.70	13.90	25.60
n	6	3	9	6
SiO ₂	36.21	36.31	36.31	36.91
TiO ₂	0.01	0.00	0.03	0.01
Al ₂ O ₃	21.05	20.10	20.26	20.57
FeO	39.49	39.29	38.37	36.67
MnO	1.53	1.18	2.22	3.81
MgO	1.89	2.16	1.90	2.42
CaO	0.24	0.23	0.30	0.35
Total	100.42	99.28	99.38	100.73
Number of atoms in formulae (oxygen basis 12)				
Si	2.955	2.995	2.993	2.991
Ti	0.001	0.000	0.002	0.001
Al	2.025	1.954	1.968	1.965
Fe	2.695	2.710	2.644	2.486
Mn	0.106	0.083	0.155	0.262
Mg	0.230	0.266	0.233	0.292
Ca	0.021	0.021	0.027	0.030
Total	8.032	8.028	8.021	8.026
Type of garnet				
Alm	87.93	87.69	86.17	80.50
Pyr	7.78	8.87	7.78	9.76
Grs	0.69	0.66	0.86	0.97
Sps	3.57	2.75	5.17	8.74
And	0.03	0.03	0.03	0.04
Ca-Ti Gt	0.00	0.00	0.00	0.00
Total	100.00	100.00	100.00	100.00

gradient the SWIR spectra were initially filtered using TSA to select only the dark mica mineral group. Two absorption features of biotite, 2,254 nm and 2,357 nm, appear to move in concert towards longer wavelengths with increasing iron content. The 2,254 nm Fe–OH absorption feature was most sensitive. Consequently, in addition to varying abundance of dark mica, a PFIT calculation on the 2,254 nm feature was used as a proxy to track variation in iron content.

The chlorite investigation used tools provided by TSA in TSG to identify variations in the abundance of Fe-, Fe–Mg- and Mg- chlorites. In addition, the wavelength of the 2,252 nm absorption feature was calculated as a geochemical gradient indicator with an increasing iron content shifting the feature to longer wavelengths (Pontual, Merry and Gamson 1997).

In the Kanmantoo data many of the calculated gradient factors showed a high degree of variance. To clarify the overall trends, a smoothing filter of a moving average over a 5 m interval was applied.

Results

The trends identified from the six mineral species showed systematic changes moving from distal to proximal locations in relation to copper mineralisation. The results of two holes (Fig. 4) were chosen to best illustrate the patterns of mineralogical changes within 300 m of mineralisation.

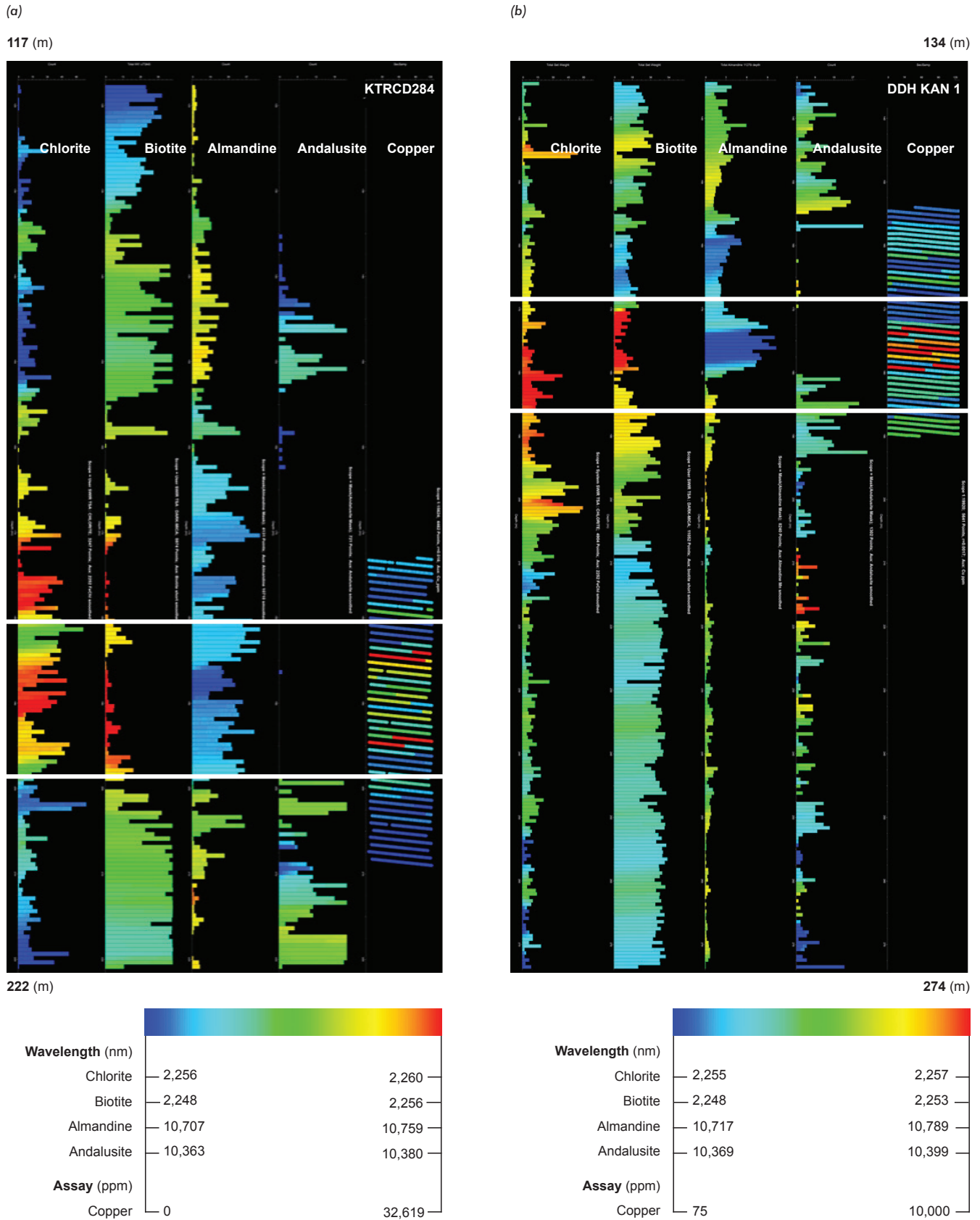
White mica (not shown) tends to be far-distal to mineralisation – up to 300 m away from copper – and absent closer. Where the chemistry of the white mica tends towards phengitic composition there is some association with gold mineralisation in late stage structures.

Andalusite is present mostly inboard of white mica but remains near-distal to the copper mineralisation, i.e. it is not usually found in close proximity to copper. The distribution of kaolinite appears to be antithetic to andalusite and is not related directly to copper mineralisation.

Electron microscopy of samples from KTDD149 confirmed dissolution and kaolinisation of andalusite was more intensive below the zone of copper mineralisation at ~280–340 m. Small clusters of poorly define jarosite crystals were associated with thin kaolinite coatings on mineral grains throughout the drillhole.

Almandine has greater abundance proximal to mineralisation and the wavelength of the 10,710 nm absorption feature trends to shorter wavelengths closer to copper.

For biotite, both the 2,254 nm (short) and the 2,356 nm (long) absorption features move in



205092_020

Figure 4 Pattern of mineral associations surrounding copper mineralisation at the Kanmantoo deposit. Horizontal lines approximate position of mineralised zone. (a) KTRCD284, (b) DDH KAN 1. Colour wavelength variables have had a 5 m moving average smoothing algorithm applied. Histogram 0.5 m bins showing relative abundance.

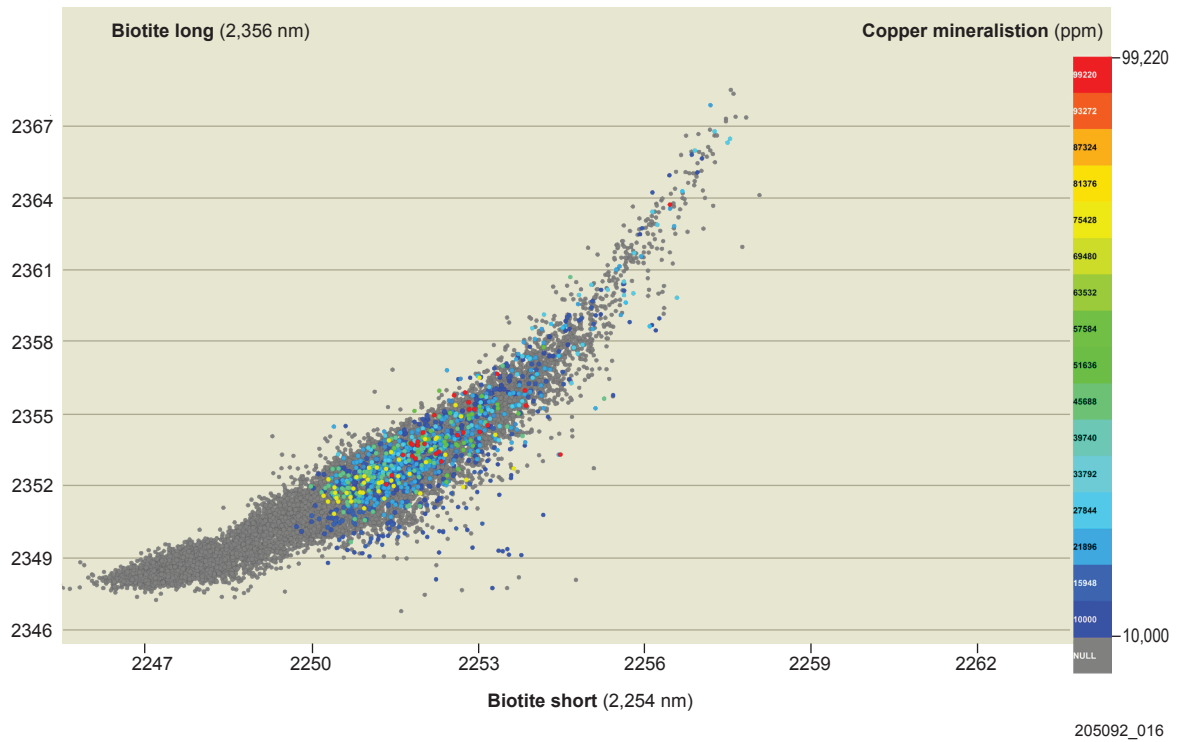


Figure 5 Relationship between wavelength of the absorption minima for the 2,254 nm and 2,357 nm of biotite in relation to copper mineralisation shown by coloured points, KTDD149.

concert and copper is associated with longer wavelengths, and with an overall decrease in biotite abundance (Fig. 5).

For chlorite the chemical gradient is towards more iron-rich species being associated with copper mineralisation.

Discussion

The combination of varying mineral abundance and change in mineral chemistry for key minerals identified from spectral data provides an indication of geochemical gradients that show a correspondence with proximity to copper mineralisation for the Kanmantoo copper orebodies. The absolute values vary from one drillhole to the next but evidence of a geochemical gradient is consistently observed. In hydrothermal systems, chemical change signalled by the presence of a geochemical gradient may be significant in ore forming processes, irrespective of the magnitude of the gradient (Keith Scott, CSIRO, pers. comm., 1997).

In the case of garnet, the shift in wavelength of the 10,710 nm absorption feature suggests a proximal almandine and more distal spessartine composition, although an increase in andalusite content and overlap of spectral features may be a factor in the apparent longer wavelengths of absorption for more distal garnet. Irrespective of the explanation, the

gradient remains consistent with longer wavelength features for garnet being distal and shorter proximal. The increase in garnet content proximal to mineralisation appears to be at the expense of andalusite and biotite.

Andalusite dissolution with associated kaolinite precipitation (Fig. 6) is interpreted as the result of a relatively low-temperature acidic fluid, post copper mineralisation. Topotactic crystallisation of kaolinite on biotite, aligned along biotite cleavage (Fig. 7) is consistent with alteration by a late hydrothermal fluid. The relatively minor kaolinite/jarosite alteration is not considered to be part of the copper mineralising system, but may be indirectly related in that the same fluid pathways were accessed and the acidity due to partial oxidation/dissolution of sulfides in this part of the system.

An outcome of the observations described above is a decision tree that incorporates spectral analysis to inform a future drill program (Fig. 8). The two gradients being measured are: (i) relative mineral abundance; and (ii) relative change in mineral chemistry. Moving through the diagram from left to right and top to bottom the presence of white mica places the sample distal to copper mineralisation by the order of 200 m. If the white mica shows a shift in the wavelength of the 2,200 nm feature (2200W) towards phengitic composition, gold may be associated. If white mica is absent but andalusite is present this places the sample in-board of white

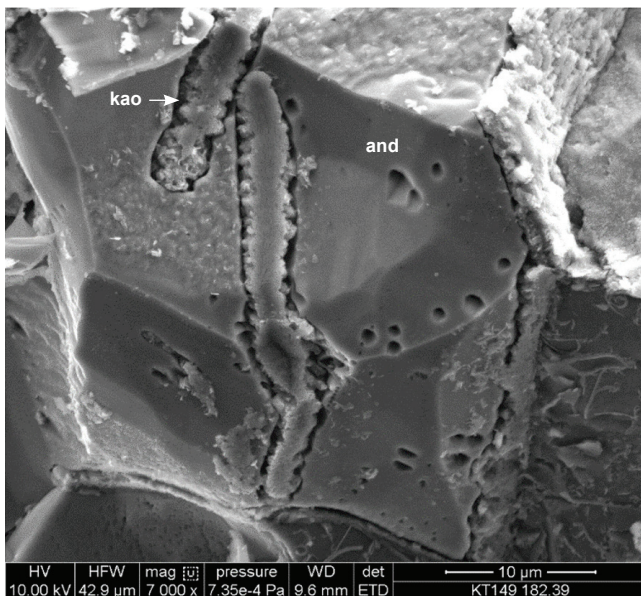


Figure 6 Electron micrograph of dissolution features in andalusite (and) partially infilled with kaolinite (kao), KTDD149, 182.39 m. (Photo 416786)

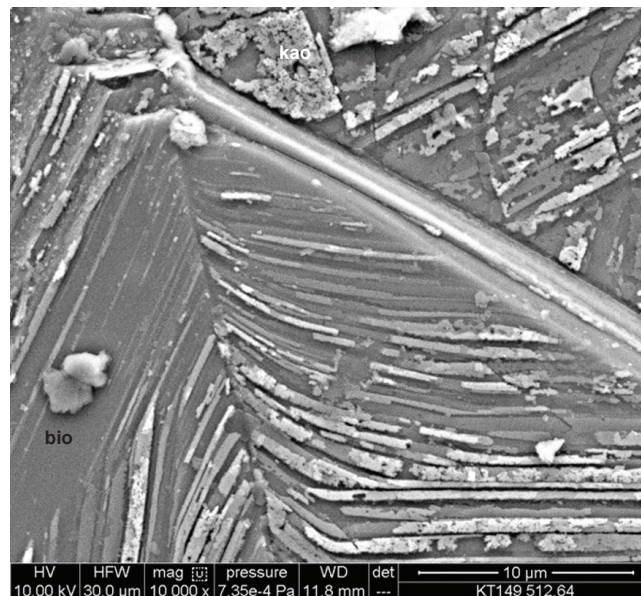


Figure 7 Electron micrograph of topotactic crystallisation of kaolinite (kao) on biotite (bio) aligned along biotite cleavage, KTDD149, 512.64 m. (Photo 416787)

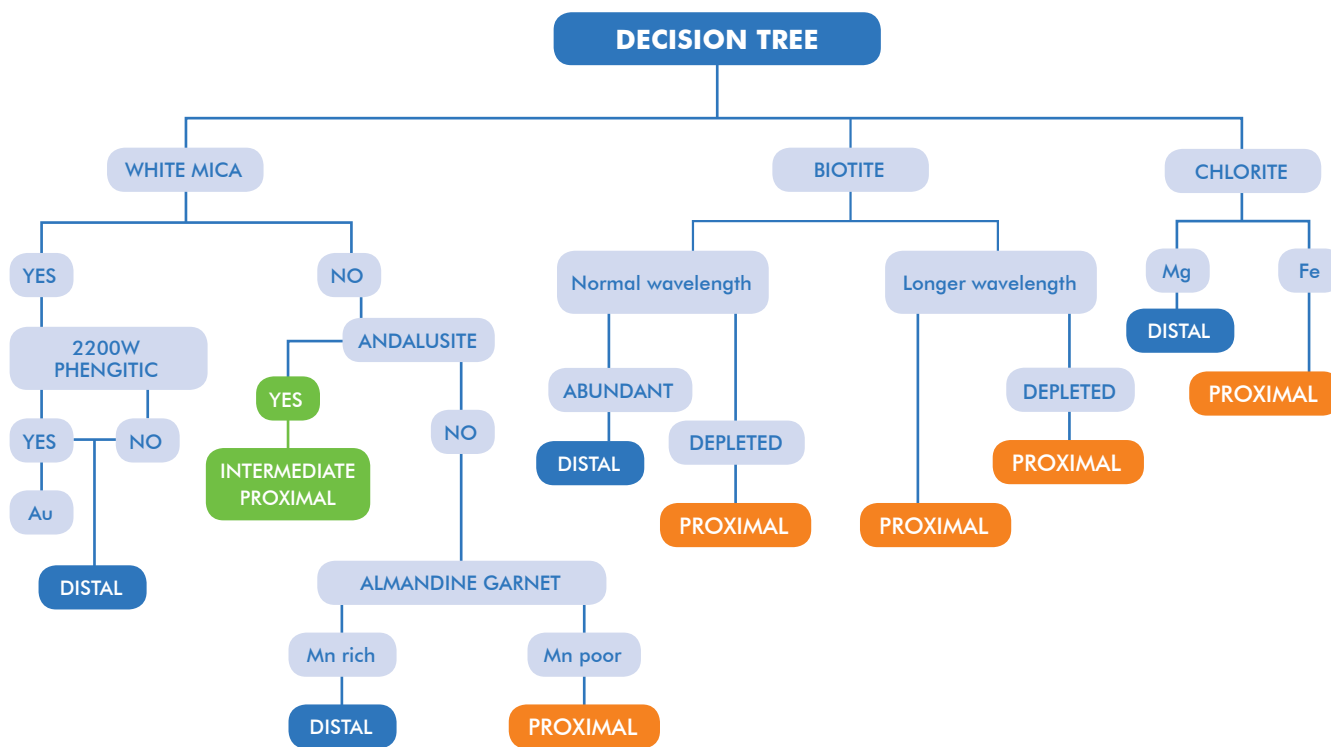


Figure 8 Decision tree to assist in the appraisal of proximity to copper mineralisation near the Kanmantoo copper deposit.

mica but still distal to mineralisation. In-board of andalusite, almandine garnet, Fe rich and Mn poor, forms proximal to mineralisation. Examining the more pervasive biotite and chlorite species, the shift to longer wavelengths of key absorption features is indicative of iron enrichment. In addition to the change in chemistry, biotite also is usually less abundant proximal to mineralisation.

Conclusion

The spectral mineralogy study of the near-mine environment at the Kanmantoo copper deposit identified geochemical/mineral gradients defined by mineral associations showing consistent patterns proximal to copper mineralisation. Useful minerals for spectral analysis included kaolin/jarosite, white mica, biotite, andalusite, almandine and chlorite.

A geochemical gradient of increasing iron content in biotite, garnet and chlorite most closely correlates with zones of copper mineralisation. Mineralogical changes in proximity to sulfide mineralisation include increased almandine abundance at the expense of andalusite and biotite.

The persistent presence of kaolinite/jarosite alteration is interpreted to result from circulation of a moderately low temperature hydrothermal fluid at comparatively shallow crustal level. This may be associated with the mineralisation, or alternatively is a younger fluid event, but either are consistent with late stage hydrothermal activity of a mineral system that developed post-metamorphism. Spectral results, however, provide few additional insights on the origin of the copper mineralisation.

Continuous spectral data of drill samples using the HyLogging system was shown to be effective in identifying patterns in the mineralogy that have consistent spatial relationship with known copper mineralisation. Consequently, this offers a useful tool that could be applied systematically to the interpretation of future drill sampling in the vicinity of the Kanmantoo Mine.

Acknowledgements

The HyLogging system refers to a group of instruments developed by CSIRO for hyperspectral measurement and imaging of mineral specimens. The trademark is now owned by Corescan Pty Ltd. TSG and TSA remain the trademarks of CSIRO. National Collaborative Research Infrastructure Strategy (NCRIS) funding, managed by AuScope, enabled the acquisition of the HyLogger 3-3 owned and operated by the Geological Survey of South Australia.

Sam Williams and Georgina Gordon (Geological Survey of South Australia) are gratefully

acknowledged for contributing to the acquisition and preliminary processing of the Kanmantoo HyLogger spectral data. Stuart McClure assisted with SEM analyses at Adelaide Microscopy.

References

- Arbon H 2011. Bismuth distribution in the Cu-Au mineralisation of the Kanmantoo deposit, South Australia. Hons thesis, University of Adelaide.
- Belperio AP, Preiss WV, Fairclough MC, Gatehouse CG, Gum J, Hough J and Burt A 1998. Tectonic and metallogenic framework of the Cambrian Stansbury Basin – Kanmantoo Trough, South Australia. *AGSO Journal of Australian Geology and Geophysics* 17:183–200.
- Both RA 1990. Kanmantoo Trough — geology and mineral deposits. In FE Hughes ed., *Geology of the mineral deposits of Australia and Papua New Guinea*. Australasian Institute of Mining and Metallurgy, Melbourne, pp.1195–1203.
- Flöttmann T, James PR, Rogers J and Johnson T 1994. Early Palaeozoic foreland thrusting and basin reactivation at the Palaeo-Pacific margin of southeastern Australia Precambrian craton: a reappraisal of the structural evolution of the southern Adelaide fold-thrust belt. *Tectonophysics* 234:95–116.
- Foden JD, Elburg MA, Dougherty-Page J and Burt A 2006. The timing and duration of the Delamerian Orogeny: correlation with the Ross Orogen and implications for Gondwana assembly. *The Journal of Geology* 114:189–210.
- Foden JD, Elburg MA, Turner SP, Sandiford M, O’Callaghan J and Mitchell S 2002. Granite production in the Delamerian Orogen, South Australia. *Journal of the Geological Society* 159:557–575.
- Gum J 1998. The sedimentology, sequence stratigraphy and mineralisation of the Silverton Subgroup, South Australia. PhD thesis, University of South Australia, Adelaide.
- Haines PW, Jago JB and Gum J 2001. Turbidite deposition in the Cambrian Kanmantoo Group, South Australia. *Australian Journal of Earth Sciences* 48:465–478.
- Hillgrove Resources Limited 2018. *Hillgrove Resources annual report for the year ended 31 December 2017*. Hillgrove Resources Limited, Adelaide.
- Kim YH, Choi S-G, Seo J, Ko K-B, Lee YJ 2018. Application of SWIR spectrometry to the determination of biotite compositions in hydrothermally altered units of the Yangyang iron-oxide-apatite (IOA) deposit, South Korea. *Ore Geology Reviews* 99:303–313.
- Lyons N 2012. Evidence for magmatic hydrothermal mineralisation at Kanmantoo copper deposit, South Australia. Hons thesis, University of Adelaide.
- McPherson MV 2017. The origin of the sediment-hosted Kanmantoo Cu-Au deposit, South Australia: mineralogical considerations. MSc Thesis, Iowa State University, Ames, Iowa.
- Offler R and Fleming PD 1968. A synthesis of folding and metamorphism in the Mt Lofty Ranges, South Australia. *Journal of the Geological Society of Australia* 15:245–266.

- Oliver NHS, Dipple GM, Cartwright I and Schiller J 1998. Fluid flow and metasomatism in the genesis of the amphibolite-facies, pelite-hosted Kanmantoo copper deposit, South Australia. *American Journal of Science* 298:181–218.
- Pollock MV, Spry PG, Tott KA, Koenig A, Both R and Ogierman J 2018. The origin of the sediment-hosted Kanmantoo Cu-Au deposit, South Australia: mineralogical considerations. *Ore Geology Reviews* 95:94–117.
- Pontual S, Merry N and Gamson P 1997. *Spectral interpretation field manual*, Vol 1, P1-84. G-Mex Version 1.0. AusSpec International Pty Ltd, Melbourne.
- Rolley P and Wright M 2017. Kanmantoo copper deposits. In GN Phillips ed., *Australian ore deposits*. The Australian Institute of Mining and Metallurgy, Melbourne, pp. 667–670.
- Sandiford M, Fraser G, Arnold J, Foden J and Farrow T 1995. Some causes and consequences of high-temperature, low-pressure metamorphism in the eastern Mt Lofty Ranges, South Australia. *Australian Journal of Earth Sciences* 42:233–240.
- Schiller JC 2000. Structural geology, metamorphism and origin of the Kanmantoo copper deposit, South Australia. PhD thesis, University of Adelaide.
- Schodloc MC, Green A and Huntington J 2016. A reference library of thermal infrared mineral reflectance spectra for the HyLogger-3 drill core logging system. *Australian Journal of Earth Sciences* 63:941–949.
- Schodloc MC, Whitbourn L, Huntington J, Mason P, Green A, Berman M, Coward D, Connor P, Wright W, Jollivet M and Martinez R 2016. HyLogger-3, a visible to shortwave and thermal infrared reflectance spectrometer system for drill core logging: functional description. *Australian Journal of Earth Sciences* 63:929–940.
- Secombe PK, Spry PG, Both RA, Jones MT and Schiller JC 1985. Base metal mineralization in the Kanmantoo Group, South Australia: a regional sulfur isotope study. *Economic Geology* 80:1824–1841.
- Spry PG, Schiller JC and Ross RA 1988. Structure and metamorphic setting of base metal mineralisation in the Kanmantoo Group, South Australia. *The AusIMM Bulletin and Proceedings* 293:57–65.
- Tedesco A 2009. Late-stage orogenic model for Cu-Au mineralisation at Kanmantoo mine: new insights from titanium in quartz geothermometry, fluid inclusions and geochemical modelling. *Journal of Geochemical Exploration* 101:103.
- Totterf S 1999. *Cambrian sediment-hosted exhalative base metal mineralisation, Kanmantoo Trough, South Australia*, Report of Investigations 57. Geological Survey of South Australia, Adelaide.
- Verwoerd PJ and Cleghorn JH 1975. Kanmantoo copper orebody. In CL Knight ed., *Economic Geology of Australia and Papua New Guinea*. Australasian Institute of Mining and Metallurgy, Melbourne, pp. 560–565.

FURTHER INFORMATION

Alan Mauger
Alan.Mauger@sa.gov.au

Building the Coompana Province

Tom Wise¹, Rian Dutch^{1, 2}, Mark Pawley¹, Clive Foss³ and Stephan Thiel^{1, 2}

¹ Geological Survey of South Australia, Department for Energy and Mining

² School of Physical Sciences, University of Adelaide ³ CSIRO

Introduction

The Coompana Province is a completely buried crustal block that occurs at the nexus of the West, South and North Australian cratons. However, very little is known about the region. The Geological Survey of Western Australia drilled a series of holes into the westernmost part of the province, which provided some insights into the architecture and geological history (Spaggiari and Smithies 2015). Yet this left a large part of the province as unknown. This was addressed with a recent program to acquire and interpret geological, geochemical and geophysical data for the Coompana Province in western South Australia (Fig. 1). Results and some interpretations have been released in a recent [MESA Journal article](#) and a [workshop abstract volume](#) (Dutch, Pawley et al. 2018; Dutch, Wise et al. 2018). This paper will expand on these publications and present the broader implications of the work that was undertaken in the Coompana Province. Whilst insights into the geology of the eastern Coompana Province have been hinted at with existing data from sparse drilling (Neumann and Korsch 2014; Fraser and Neumann 2016; Travers 2015) and correlations with the western Coompana, Madura and Musgrave provinces, the eastern Coompana Province was still a gap in the understanding of Proterozoic Australia (Fig. 2; Spaggiari et al. 2015).

Data acquisition in the South Australian part of the Coompana Province commenced in 2013 with the 13GA-EG1 seismic line, linking the central Gawler Craton, with the Albany–Fraser Orogen in Western Australia (Dutch, Pawley and Wise 2015). The seismic line imaged, for the first time, the architecture of the western margin of the Gawler Craton and the contact with the largely unknown basement rocks of the Coompana Province (Doublier et al. 2015). Complementing the deep-crustal imaging seismic line was a co-located broadband magnetotellurics (MT) profile (Thiel, Wise and Duan 2015; Thiel, Wise and Duan 2018). In the Coompana Province the seismic and MT

profiles image a complex story of major crustal-scale structures and extensional fabrics exploited and overprinted by multiple generations of intrusive magmatism (Pawley, Wise, Dutch et al. 2018; Thiel, Wise and Duan 2018; Wise and Thiel 2018).

Regional potential field surveys were acquired in 2015 (aeromagnetism and radiometrics; Heath, Reed and Katona 2015) and 2017 (ground gravity; Heath and Wise 2017). Preliminary interpretation of the aeromagnetic imagery showed a number of broad geophysical domains and possible reversely magnetised intrusions (Wise, Pawley and Dutch 2015) that would be the focus of the 2017 Coompana Drilling Project (Fig. 3; Dutch, Pawley et al. 2018).

Geological, geochemical and geophysical characterisation of the thickness, extent and nature of the cover sequences blanketing the entirety of the Coompana Province (Dunn and Waldron 2014; Foss et al. 2018; Gonzalez-Alvarez et al. 2018; Heath et al. 2018; Krapf and Gonzalez-Alvarez 2018; Meixner et al. 2018; Noble et al. 2018) aided in the planning of the Coompana Drilling Project, and provided fundamental datasets in this poorly understood region.

In this paper we will synthesise the results of the large body of precompetitive data acquired (Dutch, Pawley et al. 2018; Dutch, Wise et al. 2018) and propose a geological framework of the basement to the eastern Coompana Province. We will also present a model for the formation of the prominent and enigmatic Coompana Magnetic Anomaly, and discuss the metallogenic potential of the region.

Geological framework

The Coompana Drilling Project (Fig. 3; Dutch, Pawley et al. 2018) provided fundamental geological controls that could be used to constrain the geophysical interpretations (e.g. seismic: Pawley, Wise, Dutch et al. 2018; and aeromagnetism: Wise, Pawley and Dutch 2015). The lithological and

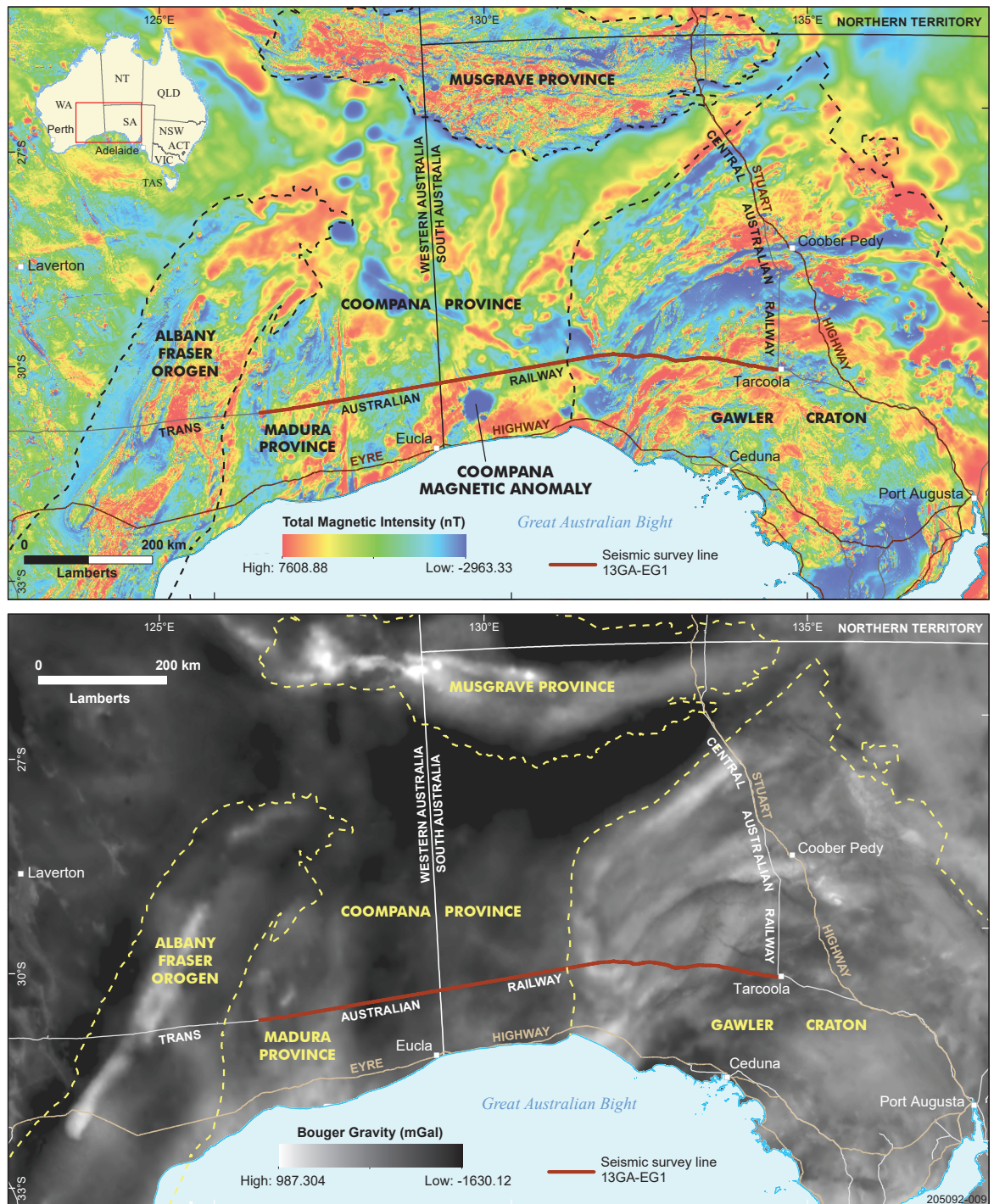
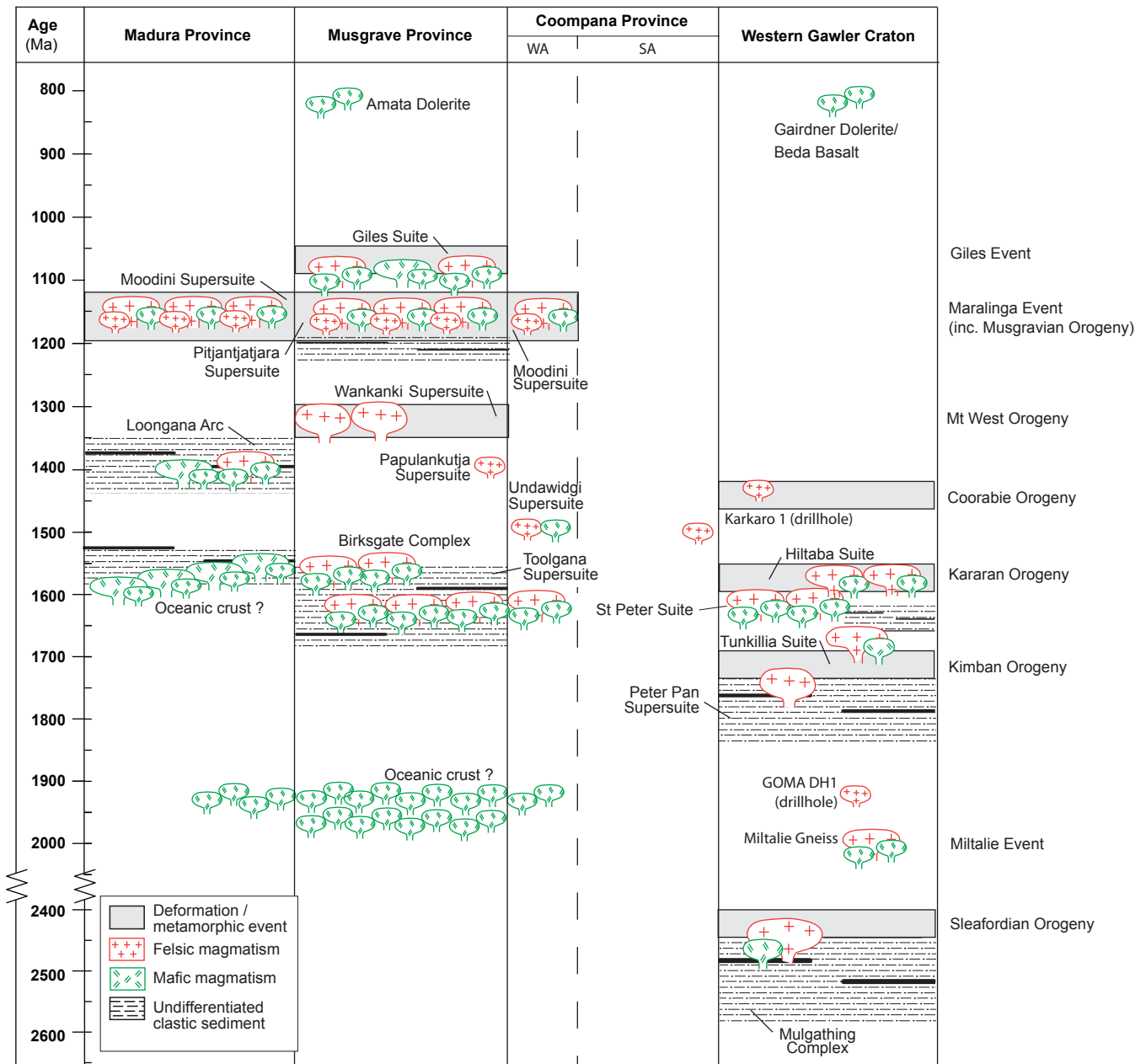


Figure 1 Regional total magnetic intensity and Bouguer gravity images showing the location of the Coompana Province with respect to the surrounding geological provinces. Also highlighting the large reversely polarised Coompana Magnetic Anomaly.

petrographical information in the drill core (Pawley, Wise, Jagodzinski et al. 2018) was combined with geochronology (Jagodzinski and Bodorkos 2018) to create a stratigraphy (Wise, Pawley and Dutch 2018a). Geochemical and isotopic analysis of the core then allowed the geological history of the region to be unravelled (Dutch 2018; Hartnady et al. 2018). Potential field datasets were then used to

determine the spatial extents of the units, resulting in an interpretive solid geology map (Fig. 4; Wise, Pawley and Dutch 2018b). Fundamentally, the evolution of the eastern Coompana Province can be divided into four main geodynamic events (Fig. 5), which are summarised in this section. For more detail, the reader is referred to Dutch, Wise et al. (2018).



205092_013

Figure 2 Time-space plot showing regional correlations in magmatic-sedimentation-deformation events, and the pre-existing knowledge gap in the South Australian section of the Coompana Province (compiled from: Dutch, Pawley and Wise 2015; Fraser and Neumann 2016; Wingate et al. 2015a, 2015b; Spaggiari and Smithies 2015; Neumann and Korsch 2014).

1 Oceanic crust development

Nd and Hf isotope data from the Coompana Province (Dutch 2018; Hartnady et al. 2018; Kirkland et al. 2017) have revealed a putative c. 2000–1900 Ma mantle extraction event that appears to be consistently represented in rocks from across the province and the neighbouring Musgrave and Madura provinces. As signatures of this event appear relatively time-constrained and of a juvenile nature, Hartnady et al. (2018) and Kirkland et al. (2017) interpret this event to represent oceanic crust development outboard of the Gawler Craton in the period c. 2000–1900 Ma, with the crust subsequently reworked and destroyed during later magmatism.

2 Prolonged arc-subduction cycles

The oldest rocks dated in the Coompana Province are the c. 1618 Ma Koomalboogurra Suite, of the Toolgana Supersuite (Dutch 2018; Jagodzinski and Bodorkos 2018; Wingate et al. 2015a). The monzogranitic orthogneisses are comparable in age and geochemistry to the St Peter Suite in the southern Gawler Craton, and have been interpreted to represent subduction-related granites, developed on the edge, or outboard of the Gawler Craton (Dutch 2018; Swain et al. 2008). The c. 1526 Ma migmatitic orthogneisses of the Bunburra Suite represent a newly reported magmatic event in this region, with juvenile isotopic character and primitive

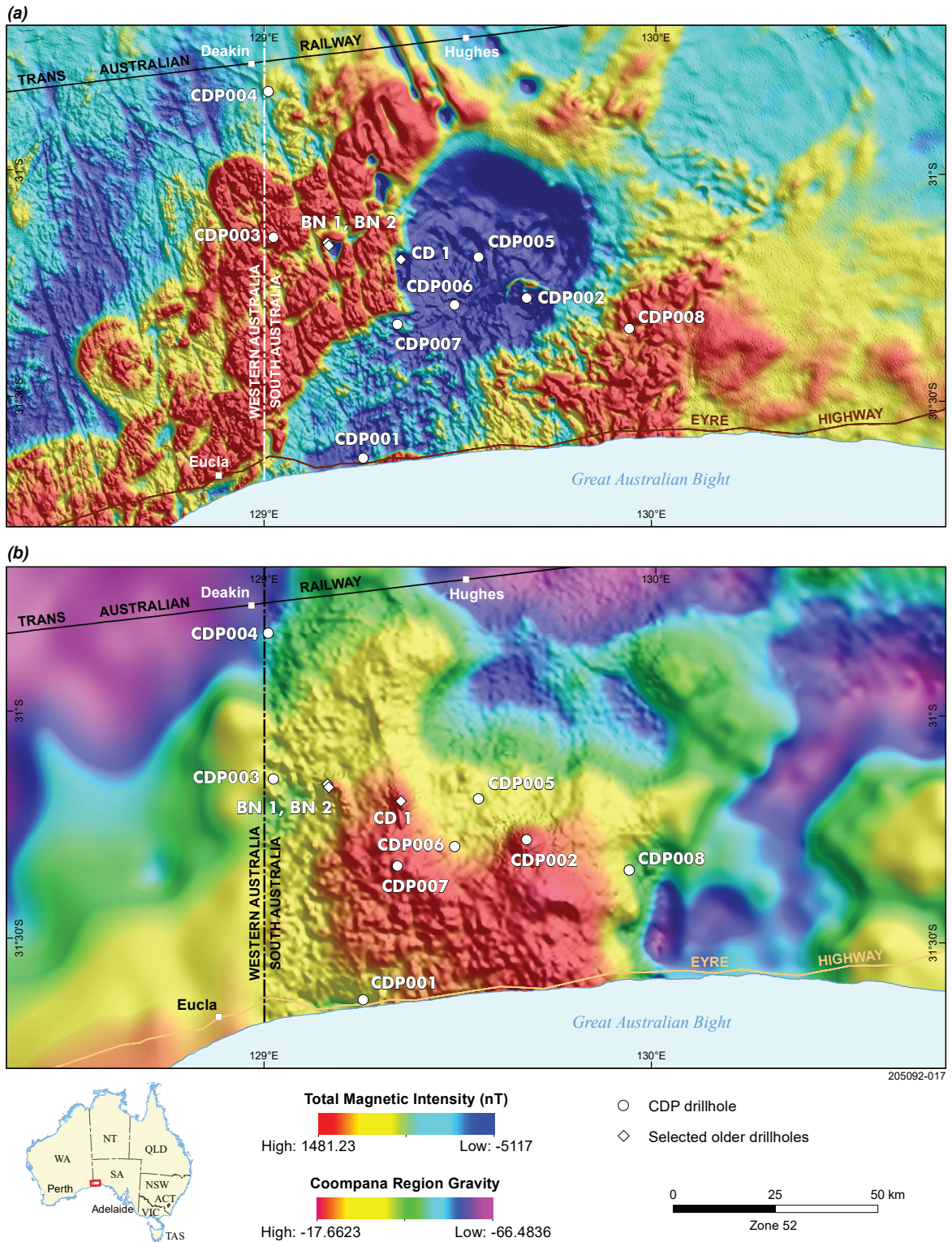


Figure 3 Location of the eight Coompana Drilling Project holes shown over (a) reduction to pole TMI image from the new Coompana magnetic survey; and (b) combination regional and new Coompana gravity survey data.

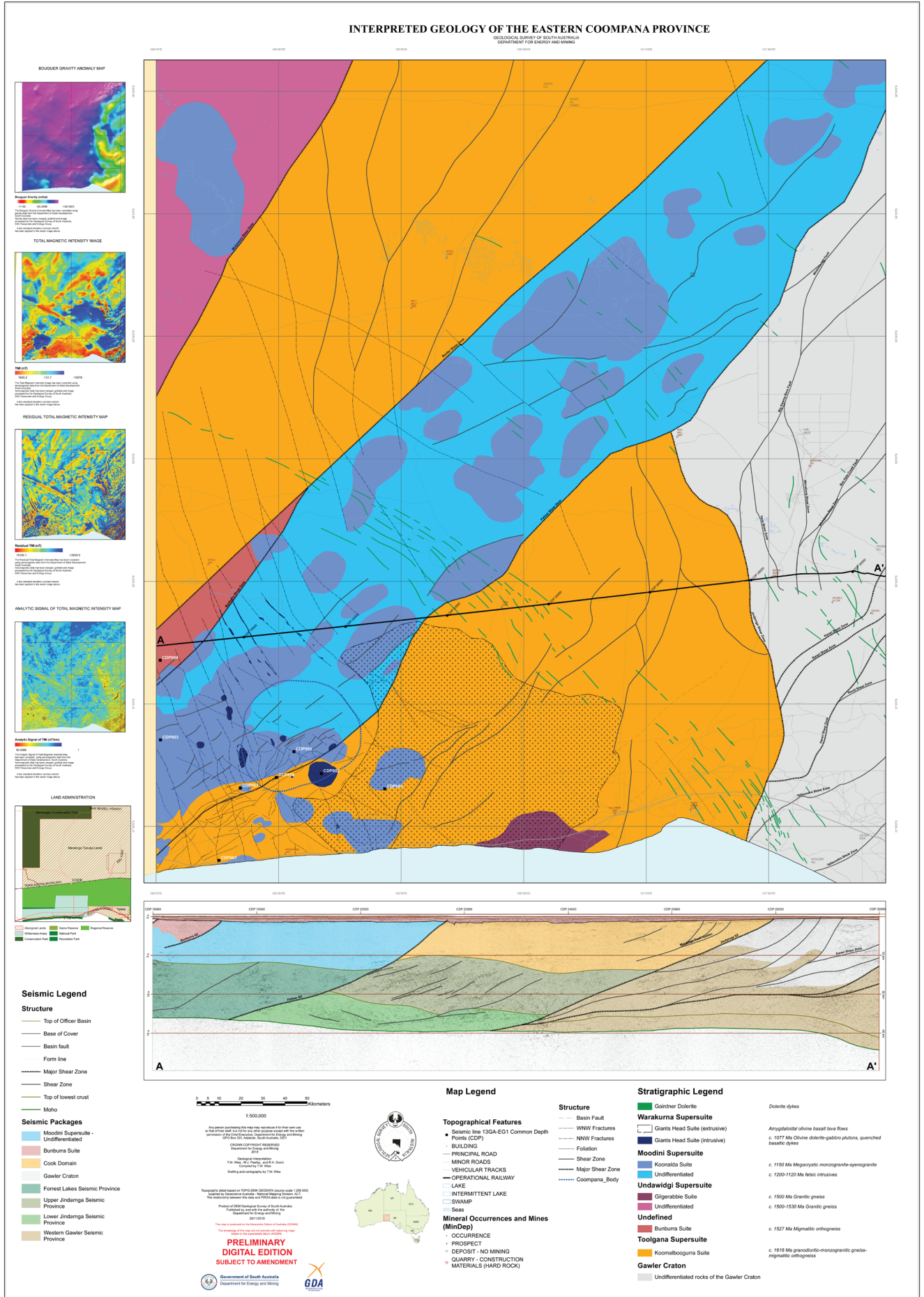


Figure 4 Interpreted geology map of the eastern Coompana Province (Wise, Pawley and Dutch 2018b).

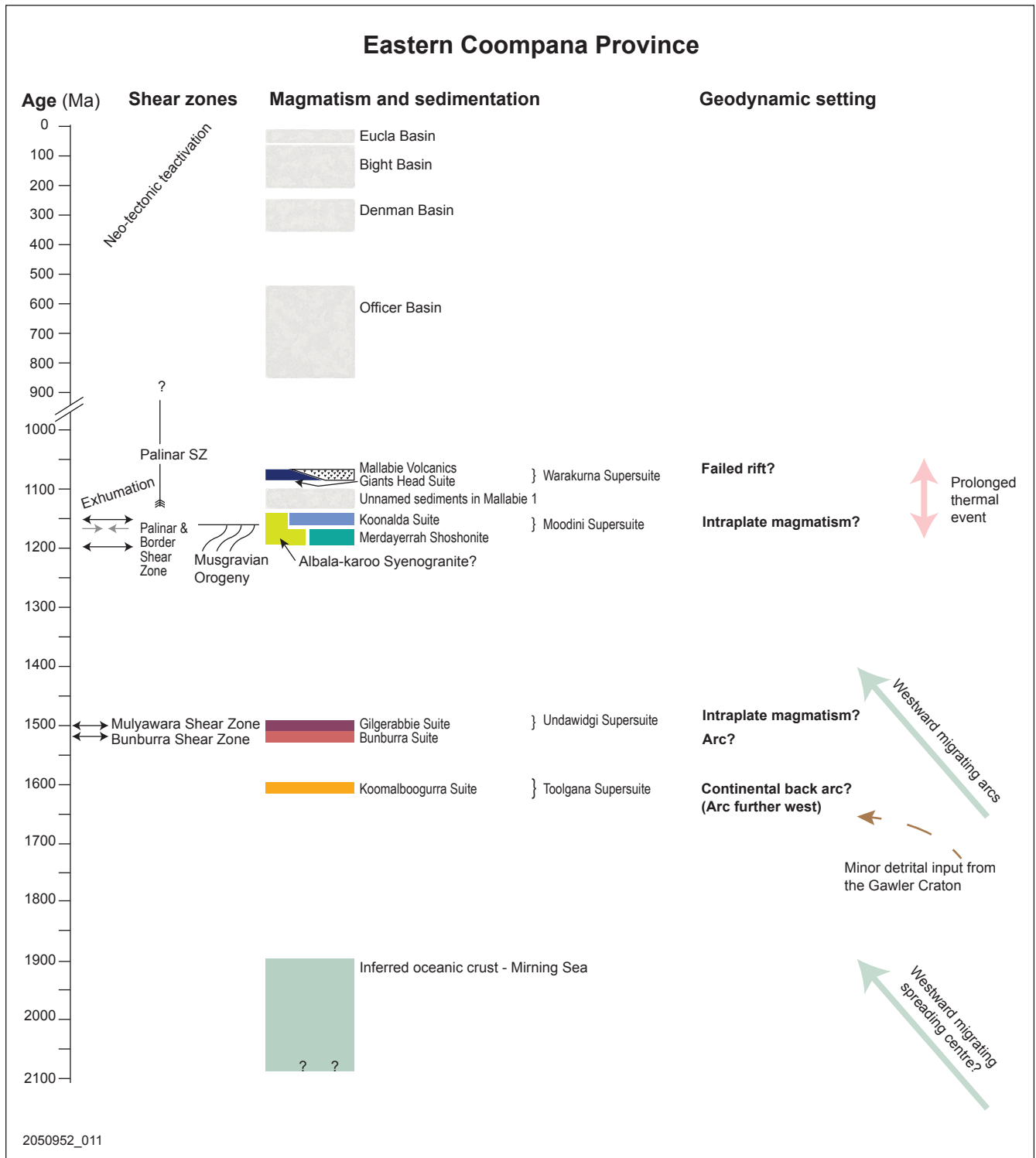


Figure 5 Geodynamic 'event' plot for the eastern Coompana Province compiled from the results presented in Dutch, Wise et al. (2018).

geochemical signatures (Dutch 2018; Jagodzinski and Bodorkos 2018). Dutch (2018) interprets the Bunburra Suite to be derived from a subduction-enriched lithospheric mantle source.

The A-type c. 1505–1487 Ma Undawidgi Supersuite (Wingate et al. 2015a), including the newly named Gilgerabbie Suite in the eastern Coompana Province (Wade et al. 2007), is interpreted to be the magmatic product of intracontinental extension (Smithies et al. 2015) after cessation of subduction in the older, c. 1526 Ma event.

As age constraints on the subduction-related rocks (above) appear to young from east to west – c. 1618 Ma in the east, to c. 1400 Ma and c. 1390 Ma in the west (Madura Province: Smithies et al. 2015; Wingate et al. 2015b; Musgrave Province: Smithies et al. 2010) – we interpret the Coompana and Madura provinces to have their origin in broadly westward-migrating (i.e. back-stepping), approximately north–south-trending arc ribbons developed on the proposed oceanic crust between the Gawler Craton and Yilgarn Craton (Dutch et al. 2016).

3 Intracontinental meltdown

In the period c. 1200–1070 Ma, magmatic rocks with a wide variety of lithology, age and compositions were intersected in drillholes of the Coompana Drilling Project (Dutch, Wise et al. 2018).

1189–1141 Ma

- undifferentiated anatectic granites in CDP001 and CDP004
- c. 1174 Ma foliated Merdayerrah Shoshonite in CDP004
- c. 1150 Ma massive porphyritic monzo- to syenogranitic intrusions of the Koonalda Suite in CDP003 and CDP005
- equigranular biotite micro-syeno- to monzogranitic Albala-karoo Syenogranite, forming late crosscutting intrusions in CDP003 and CDP005
- peraluminous Nb-, Ta-enriched granite dykes in CDP001.

c. 1074 Ma

- quenched basalt dykes composed of primarily plagioclase with clinopyroxene, opaques and mesostasis (dykes in CDP003 and CDP006)
- olivine basalts (intrusive rock in CDP002, extrusive rock in CDP008 and CD 1)
- two-pyroxene basalts (intrusive rocks in CDP007, BN2 and BN1).

The relatively juvenile $\epsilon_{\text{Hf}}1174\text{--}1140$ Ma values of the Merdayerrah Shoshonite and Koonalda Suite melts suggest little or no assimilation of any pre-1900 Ma crust, and appear to be the product of mantle input and assimilation of crust similar to the Bunburra and Koomalboogurra suites (Dutch 2018).

In contrast, mantle melts at c. 1074 Ma (Giants Head Suite: Jagodzinski and Bodorkos 2018) show evolved (strongly negative) $\epsilon_{\text{Hf}}1074$ Ma values, indicating that contamination by a >1900 Ma crustal substrate is required (Dutch 2018). We therefore interpret a highly reflective lower crustal unit in the seismic section, coincident with the top of a subvertical mantle conductor (Fig. 6), represents a relic of possible Gawler Craton crust beneath the Coompana Province, and is the contaminant in ascending mantle melts.

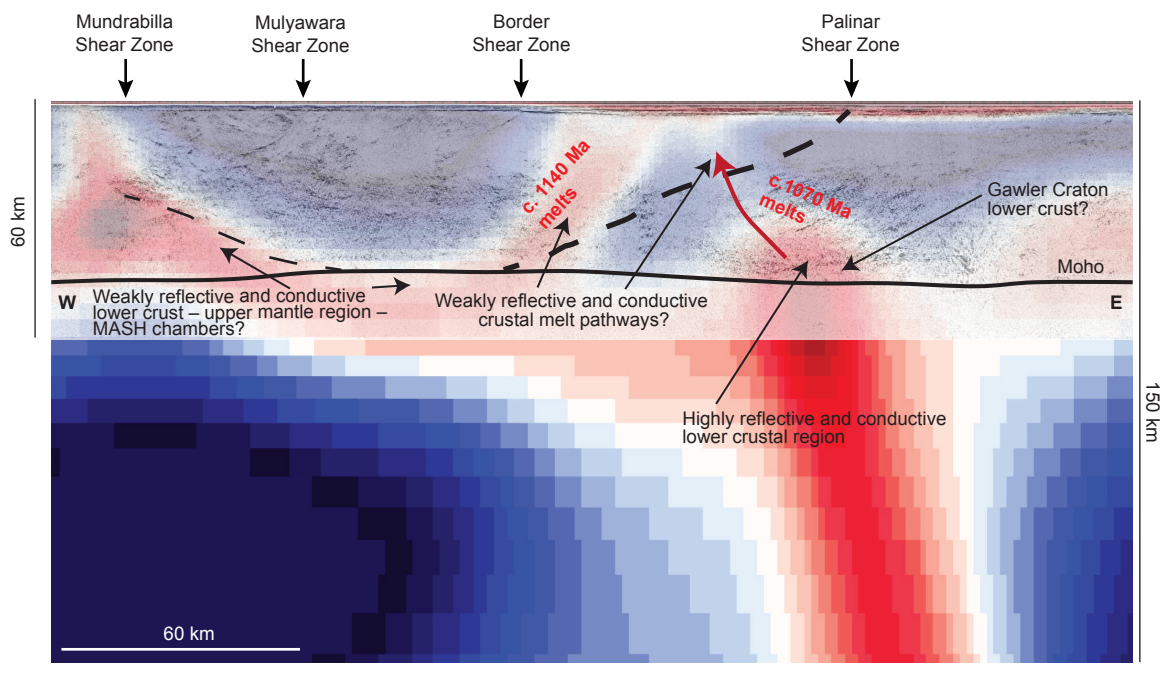
Seismic and MT signatures are interpreted to signify changing melt sources between the major periods of magmatism at c. 1140 Ma and c. 1074 Ma (Fig. 6). As c. 1140 Ma melt from extensive conductive/non-reflective lower crustal – upper mantle MASH (melting–assimilation–storage–homogenisation) chambers beneath the Coompana Province (e.g. Fig. 6) was mobilised upward, melt pathways in the hanging wall of the Palinar Shear Zone (Fig. 6) destroyed pre-existing fabrics in the mid–upper crust (e.g. Wise and Thiel 2018) and reached the near-surface, crystallising to form plutons of the Koonalda Suite (Pawley, Wise, Dutch et al. 2018; Thiel, Wise and Duan 2018).

The varied geochemical signatures exhibited by mafic rocks of the c. 1074 Ma Giants Head Suite (Dutch 2018) are suggestive of a heterogeneous lithospheric mantle. Evidenced by the significant negative gravity anomaly associated with the Coompana Province (Fig. 1), it is possible that delamination of the mafic residual components of c. 1200–1140 Ma MASH chambers in the lower crust into the lithosphere provided a catalyst for melting of heterogeneous source material for the c. 1074 Ma magmatism.

Development of thick continental lithosphere and metasomatism of the lithospheric mantle associated with c. 1620–<1500 Ma arc development, and a widespread mantle heat source at c. 1200 Ma were the likely catalysts for a >100 My period of magmatism between c. 1200 Ma and c. 1074 Ma.

4 Sedimentation

Post-dating the last major magmatic episode in the Coompana Province (1074 Ma), sedimentation in the Neoproterozoic–Cambrian Officer Basin, the Permian Denman Basin, the mid-Jurassic to late-Cretaceous Bight Basin and the Cenozoic Eucla Basin blanketed the Coompana Province.



205092_012

Figure 6 Overlain seismic section (13GA-EG1) and 2D MT inversion depicting the crustal structure and differing melt sources and pathways for c. 1140 Ma and c. 1070 Ma magmatism (modified after Pawley, Wise, Dutch et al. 2018; Thiel, Wise and Duan 2018; Wise and Thiel 2018).

Magnetic source estimates (Foss et al. 2017), cover geophysics (Heath et al. 2018; Meixner et al. 2018) and drillhole constraints suggest that the cover thickness across the southern Coompana Province is shallowest (<250 m), whilst cover thickness exceeds 1,300 m in the Denman Basin to the east, and 2,500 m in the northern Coompana Province, beneath the Officer Basin.

Coompana Magnetic Anomaly

The source of the Coompana Magnetic Anomaly, a ~50 km wide, circular, reversely polarised anomaly in the southern Coompana Province has been the topic of debate since it was first identified by widely spaced aeromagnetic data in the early 1970s. Drilling in the early 1980s targeted ~1–2 km wide satellite anomalies, with mafic volcanics and intrusive rocks being returned from below the basement unconformity (Shell Co. of Australia Ltd 1983; Carpentaria Exploration Co. Pty Ltd 1982a, 1982b). An early attempt to ascertain the age of these volcanics using Sm–Nd isochrons gave a poorly constrained age of c. 859 ± 66 Ma (Travers 2015). Accurate U–Pb dating of these mafic rocks was not possible until drillhole CDP002 (Dutch, Jagodzinski et al. 2017) returned massive olivine dolerite and microgabbro from beneath the basement unconformity. A fractionated interval close to the top of the basement interval returned a small population of zircon, and was dated with a magmatic crystallisation age at 1074 ± 6 Ma (Jagodzinski and Bodorkos 2018). The age of

these rocks indicates that they are part of the c. 1078–1070 Ma Warakurna Supersuite (Howard et al. 2011; Wingate, Pirajno and Morris 2004), significantly increasing the extent of the Warakurna Large Igneous Province (Alghamdi et al. 2018; Wingate et al. 2004). Magnetisation studies on the reversely polarised anomalies caused by the satellite bodies intersected in previous drilling and in CDP002 suggest that magnetisation directions, whilst variable, are consistent with an extended period of magmatism, rather than multiple discrete events (Foss et al. 2018). This therefore implies that satellite bodies, and the Coompana Magnetic Anomaly, are all likely to be temporally related to the CDP002 olivine dolerite–microgabbro.

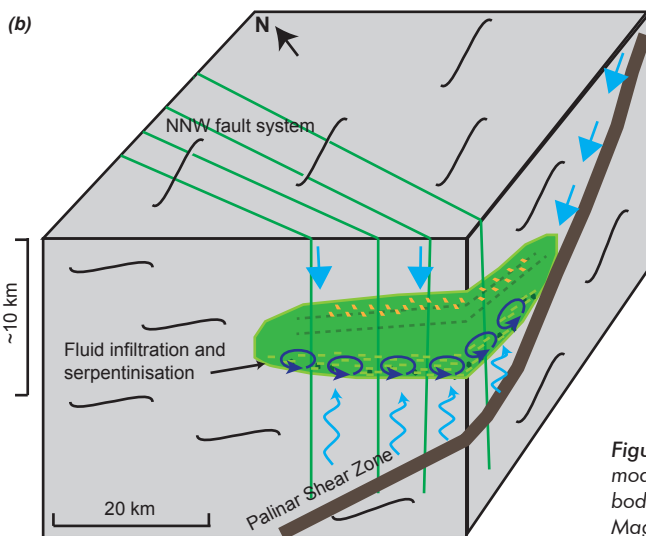
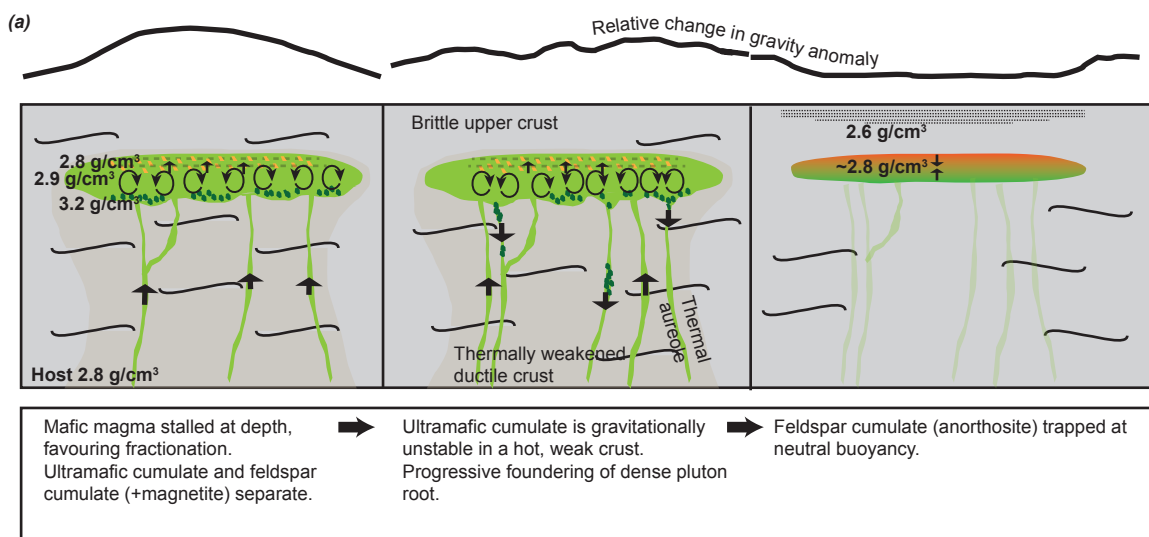
Of particular interest are the gravity and magnetic signatures of the satellite bodies and the Coompana Magnetic Anomaly. The satellite bodies have reversely polarised magnetic anomalies that are spatially associated with positive gravity anomalies, implying that the causative body is both strongly magnetic and dense, e.g. the olivine dolerite–microgabbro in CDP002. In contrast, the Coompana Magnetic Anomaly displays a similarly reversely polarised high intensity magnetic anomaly, but is not spatially associated with a positive gravity anomaly (Foss et al. 2018). As the body causing the Coompana Magnetic Anomaly is strongly magnetic, we propose that initially, this was a mafic–ultramafic body that has undergone a process to remove the high-density component.

Foundering vs serpentinisation, removal vs alteration

Whilst an increase in the thickness of a sedimentary succession is required to satisfy low-density responses at the cover–basement interface (Foss et al. 2018), a process to significantly reduce the density of a mafic–ultramafic magmatic body is required to achieve the current density-neutral state with the surrounding host rocks. In both cases, pluton differentiation and stratification is required to have concentrated a mafic–ultramafic cumulate towards the base of the magma chamber, and an upper layer of predominantly plagioclase and magnetite.

We propose two possible, not mutually exclusive, mechanisms for the apparent lack of this layer remaining in situ – foundering and serpentinisation (Fig. 7).

Foundering. As the denser cumulate phase built up, gravitational instabilities developed between the cumulate layer(s) and the less-dense granitic–gneissic host rocks within the weakened thermal aureole of the intrusion (Roman and Jaupart 2016). Negative buoyancy and associated Rayleigh-Taylor instabilities enabled the dense cumulate phase to progressively founder through feeder zones and weakened host rocks, thereby physically removing



205092_019

Figure 7 Schematic cartoons of the proposed alternative models generating the unusual signatures of the plutonic body interpreted to be the cause of the Coompana Magnetic Anomaly. (a) Foundering model, where progressive removal of a dense cumulate reduces the net density of the pluton. (b) Serpentinisation model, where fluid infiltration at the intersection of fault–shear systems alters the dense basal layer of the differentiated pluton, producing serpentinite + magnetite.

the dense material from the crystallising pluton (e.g. Glazner 1994; Roman and Jaupart 2016). As no significant long-wavelength (lower crustal) positive gravity anomaly is observed in the Coompana Province (Fig. 1), it is possible that complete removal of the founded cold, dense cumulate into the mantle was achieved.

Serpentinisation. Pervasive alteration of the mafic–ultramafic cumulate could, if on a large enough scale, reduce the density of the basal layer to the plutonic body, whilst also generating magnetite, required for the high-intensity magnetic anomaly. Such alteration would require significant volumes of fluid to produce serpentinite on this scale. The Coompana body sits at the intersection of the crustal-scale Palinar Shear Zone and a significant NW–NNW-trending structure set. Fluids may have been focused at the intersection of these structures, enabling serpentinisation. Significant pre- and post-magmatic hydrothermal alteration is observed within the Palinar Shear Zone to the southwest (CDP006; Pawley, Wise, Jagodzinski et al. 2018).

Metallogenic implications

The program of data acquisition in the Coompana Province has implications for the prospectivity of the region, as prior to 2013, the sum total of prospectivity indicators were some interesting, but poorly resolved geophysical anomalies in a region entirely blanketed by sedimentary cover. Systematic data acquisition and development of the geological framework described above has identified several factors that raise the prospectivity of the region:

- The cover thickness has been constrained by drillholes and multiple geophysical techniques (Foss et al. 2017, 2018; Meixner et al. 2018). Cover thickness is less than 400 m for a large region in the southern Coompana Province, and decreases to ~200 m in places, highlighting the accessibility of the basement rocks.
- Major crustal-scale shear zones cross the Coompana Province, and are interpreted to represent boundaries between lower crustal units of differing ages and compositions (Dutch 2018; Pawley et al. 2018). Domain-bounding structures have been strongly linked to the spatial location of mineral deposits in places such as the Yilgarn Craton (Mole et al. 2013). Significant poly-phase hydrothermal alteration is observed in drillhole CDP006, located within one such structure, the Palinar Shear Zone (Dutch, Pawley et al. 2017; Pawley, Wise, Dutch et al. 2018; Pawley, Wise, Jagodzinski et al. 2018).
- Geochronology has revealed that mafic rocks of the Giants Head Suite (Dutch 2018; Jagodzinski and Bodorkos 2018; Wise, Pawley and Dutch 2018a) are temporal equivalents of the Giles Complex in the Musgrave Province, and part

of the larger Warakurna Supersuite. The Giles Complex is host to the Nebo-Babel deposit in the western Musgrave Province (Godel et al. 2011). The temporal (and genetic) association with the Giles Complex raises the Ni–Cu – platinum group elements potential of the Giants Head Suite.

- Shoshonitic magmatism (CDP004, c. 1170 Ma Merdayerrah Shoshonite; Dutch 2018; Jagodzinski and Bodorkos 2018; Pawley, Wise, Jagodzinski et al. 2018; Wise, Pawley and Dutch 2018a) provides a link between previously enriched lithospheric mantle and the crustal magmatism. Magmatism with shoshonitic affinities has been found to be associated with Cu/Cu–Au deposits globally (e.g. Bingham Canyon Cu–Au–Mo; Groves and Santosh 2015).
- Peraluminous granites from drillhole CDP001 in the southern Coompana Province (Dutch, Pawley et al. 2017) exhibit elevated Rb, Nb and Ta values, and relative depletions in Ba and Sr. These signatures are typical of biotite–muscovite granites associated with Nb–Ta mineralisation (Dutch 2018; Pollard 1989). In addition, low K/Rb ratios, typical of late-magmatic pegmatites (Shaw 1968), high F concentrations, and albite–sericite–chlorite–fluorite hydrothermal alteration assemblages, suggests a highly acidic hydrothermal fluid was able to remobilise Nb and Ta (Zaraisky, Korzhinskaya and Kotova 2010), elevating potential for these rare metals.

Conclusion

The Coompana Project represents a major precompetitive geoscience program in a covered, greenfield region which has seen very little scientific or exploration attention. The results of this significant precompetitive geoscience data acquisition program and workflow have been synthesised into a new geological and geodynamic framework that puts the Coompana Province into regional context and fills a knowledge gap in our understanding of Proterozoic Australia. From the data, we are able to recognise four main geodynamic events affecting the Coompana Province, and relate them to the surrounding Proterozoic terranes in the Musgrave and Madura provinces. The development of a geodynamic framework and broader links with surrounding metallogenic provinces have allowed us to identify key indicators of the mineral prospectivity for this previously unknown region.

References

- Alghamdi AH, Aitken ARA and Dentith MC 2018. The deep crustal structure of the Warakurna LIP, and insights on Proterozoic LIP processes and mineralisation. *Gondwana Research* 56:1–11.
- Carpentaria Exploration Co. Pty Ltd 1982a. EL 472 and EL 849, Bundulla, progress reports for the period 24/5/79 to 19/10/82, Open file Envelope O3515. Primary Industries and Resources South Australia, Adelaide.

- Carpentaria Exploration Co. Pty Ltd 1982b. EL 503 and EL 905, Koonalda, progress reports for the period 7/8/79 to 18/7/82, Open file Envelope 03604. Primary Industries and Resources South Australia, Adelaide.
- Doublier MP, Dutch RA, Clark D, Pawley MJ, Fraser GL, Wise TW, Kennett BLN, Reid AJ, Spaggiari CV, Calvert AJ, van der Wielen S, Dulfer H, Bendall BR, Thiel S and Holzschuh J 2015. Interpretation of the western Gawler Craton section of seismic line 13GA-EG1. In RA Dutch, MP Pawley and TW Wise eds, *What lies beneath the western Gawler Craton? 13GA-EG1E Seismic and Magnetotelluric Workshop 2015*, Report Book 2015/00029. Department of State Development, South Australia, Adelaide, pp. 28–40.
- Dunn CE and Waldron H 2014. *Regional biogeochemical survey of the Eucla Basin, South Australia*, Report Book 2014/00025. Department of State Development, South Australia, Adelaide.
- Dutch R 2018. Coompana Province geochemistry and petrogenesis. In R Dutch, T Wise, M Pawley and A Petts eds, *Coompana Drilling and Geochemistry Workshop 2018 extended abstracts*, Report Book 2018/00019. Department for Energy and Mining, South Australia, Adelaide, pp. 76–101.
- Dutch RA, Jagodzinski EA, Wise TW, Pawley MJ, Tylkowski L, Lockheed A, McAlpine SRB and Heath P 2017. *PACE Copper Coompana Drilling Project: Drillhole CDP002 preliminary field-data report*, Report Book 2017/00038. Department of the Premier and Cabinet, South Australia, Adelaide.
- Dutch RA, Pawley MP and Wise TW eds 2015. *What lies beneath the western Gawler Craton? 13GA-EG1E Seismic and Magnetotelluric Workshop 2015*, Report Book 2015/00029. Department of State Development, South Australia, Adelaide.
- Dutch RA, Pawley MJ, Wise TW, Jagodzinski EA, Tylkowski L, Lockheed A and McAlpine S 2018. Breaking down the Coompana Drilling Project. *MESA Journal* 87:4–14.
- Dutch RA, Pawley MJ, Wise TW, Tylkowski L, Lockheed A, McAlpine SRB and Heath P 2017. *PACE Copper Coompana Drilling Project: Drillhole CDP001 preliminary field-data report*, Report Book 2017/00022. Department of the Premier and Cabinet, South Australia, Adelaide.
- Dutch RA, Pawley MJ, Wise TW, Tylkowski L, Lockheed A, Jagodzinski EA, McAlpine SRB and Heath P 2017. *PACE Copper Coompana Drilling Project: Drillhole CDP006 preliminary field-data report*, Report Book 2017/00043. Department of the Premier and Cabinet, South Australia, Adelaide.
- Dutch R, Spaggiari CV, Doublier MP, Pawley M, Wise TW, Kennett BLN, Gessner K, Thiel S, Clark D and Holzschuh J 2016. What lies beneath the Nullarbor Plain? Insights into the geology of the Coompana Province from deep crustal seismic reflection profile 13GA-EG1. *Australian Earth Sciences Convention, 26–30 June 2016, Abstracts*, Abstract 118. Geological Society of Australia, Adelaide, p. 120.
- Dutch R, Wise T, Pawley M and Petts A 2018. *Coompana Drilling and Geochemistry Workshop 2018 extended abstracts*, Report Book 2018/00019. Department for Energy and Mining, South Australia, Adelaide.
- Foss C, Heath P, Dutch R, Wise TW, Pawley M and Reed G 2018. Coompana gravity and magnetic studies. In R Dutch, T Wise, M Pawley and A Petts eds, *Coompana Drilling and Geochemistry Workshop 2018 extended abstracts*, Report Book 2018/00019. Department for Energy and Mining, South Australia, Adelaide, pp. 41–50.
- Foss C, Reed G, Keeping T, Wise T and Dutch R 2017. *Source magnetisation studies of the reverse magnetic anomalies in the Coompana area*, Report Book 2017/00029. Department of the Premier and Cabinet, South Australia, Adelaide.
- Fraser GL and Neumann NL 2016. *Under the Nullarbor: new SHRIMP U-Pb zircon ages from the Coompana, Madura and Albany-Fraser provinces, and Officer Basin, western South Australia and eastern Western Australia: July 2014 - June 2015*, Record 2016/16. Geoscience Australia, Canberra.
- Glazner AF 1994. Foundering of mafic plutons and density stratification of continental crust. *Geology* 22:435–438.
- Godel B, Seat Z, Maier WD and Barnes S-J 2011. The Nebo-Babel Ni-Cu-PGE sulfide deposit (West Musgrave Block, Australia): Pt. 2, Constraints on parental magma and processes, with implications for mineral exploration. *Economic Geology* 106:557–584.
- González-Álvarez I, Krapp C, Fox D, Noble R, Reid N, Verrall M, Foss C, Ibrahim T, Dutch R, Jagodzinski L, Cole D, Lau I, Robertson J and Pinchand T 2018. Insights on landscape geochemistry in the Coompana region: implications for geochemical dispersion and mineral exploration through cover. In R Dutch, T Wise, M Pawley and A Petts eds, *Coompana Drilling and Geochemistry Workshop 2018 extended abstracts*, Report Book 2018/00019. Department for Energy and Mining, South Australia, Adelaide, pp. 20–27.
- Groves DI and Santosh M 2015. Province-scale commonalities of some world-class gold deposits: implications for mineral exploration. *Geoscience Frontiers* 6:389–399.
- Hartnady MIH, Kirkland CL, Dutch RA, Bodorkos S and Jagodzinski EA 2018. Zircon Hf isotopic signatures of the Coompana Province in South Australia. In R Dutch, T Wise, M Pawley and A Petts eds, *Coompana Drilling and Geochemistry Workshop 2018 extended abstracts*, Report Book 2018/00019. Department for Energy and Mining, South Australia, Adelaide, pp. 132–144.
- Heath P, Gouthas G, Irvine J, Krapp C and Dutch RA 2018. Microgravity surveys on the Nullarbor. In R Dutch, T Wise, M Pawley and A Petts eds, *Coompana Drilling and Geochemistry Workshop 2018 extended abstracts*, Report Book 2018/00019. Department for Energy and Mining, South Australia, Adelaide, pp. 33–39.
- Heath P, Reed G and Katona L 2015. 2015 Coompana airborne survey. *MESA Journal* 79:18–21. Department of State Development, South Australia, Adelaide.
- Heath P and Wise TW 2017. *Coompana Gravity Survey: download now*. In Department of the Premier and Cabinet, *MESA Journal – News 2017*, *MESA Journal News* 2017:25. Department of the Premier and Cabinet, South Australia, Adelaide.
- Howard HM, Smithies RH, Evins PM, Kirkland CL, Werner M, Wingate MTD and Pirajno F 2011. *Explanatory Notes for the west Musgrave Province*. Geological Survey of Western Australia, Perth.

- Jagodzinski EA and Bodorkos S 2018. U-Pb geochronology of the eastern Coompana Province, South Australia. In R Dutch, T Wise, M Pawley and A Petts eds, *Coompana Drilling and Geochemistry Workshop 2018 extended abstracts*, Report Book 2018/00019. Department for Energy and Mining, South Australia, Adelaide, pp. 66–75.
- Kirkland C, Smithies R, Spaggiari C, Wingate M, de Gromard RQ, Clark C, Gardiner N and Belousova E 2017. Proterozoic crustal evolution of the Eucla basement, Australia: implications for destruction of oceanic crust during emergence of Nuna. *Lithos* 278:427–444.
- Krapf C and Gonzalez-Alvarez I 2018. It is rather flat out there... Regolith mapping depicting intricate landscape patterns and relationships to bedrock geology and structures under cover on the Nullarbor Plain. In R Dutch, T Wise, M Pawley and A Petts eds, *Coompana Drilling and Geochemistry Workshop 2018 extended abstracts*, Report Book 2018/00019. Department for Energy and Mining, South Australia, Adelaide, pp. 12–17.
- Meixner T, Jiang W, Holzschuh J, Dutch RA, Pawley MP, McAlpine S, Duan J and Wise TW 2018. Comparison of pre-drilling geophysics against drilling results in the Coompana Province of South Australia. In R Dutch, T Wise, M Pawley and A Petts eds, *Coompana Drilling and Geochemistry Workshop 2018 extended abstracts*, Report Book 2018/00019. Department for Energy and Mining, South Australia, Adelaide pp. 28–32.
- Mole DR, Fiorentini ML, Cassidy KF, Kirkland CL, Thebaud N, McCuaig TC, Doublier MP, Duuring P, Romano SS, Maas R, Belousova EA, Barnes SJ and Miller J 2013. Crustal evolution, intracratonic architecture and the metallogeny of an Archaean craton. In GRT Jenkin, PAJ Lusty, I McDonald, MP Smith, AJ Boyce and JJ Wilkinson eds, *Ore deposits in an evolving earth*, Special Publication. Geological Society of London, pp. 23–80.
- Neumann NL and Korsch RJ 2014. *SHRIMP U–Pb zircon ages from Kutjara 1 and Mulyawara 1, northwestern South Australia*, Record 2014/05. Geoscience Australia, Canberra.
- Noble R, Gonzalez-Alvarez I, Reid N, Pinchand T, Cole D, Krapf C, Lockheed A, Broadbridge L and Jagodzinski EA 2018. The sampling workflow and surface geochemistry of Coompana. In R Dutch, T Wise, M Pawley and A Petts eds, *Coompana Drilling and Geochemistry Workshop 2018 extended abstracts*, Report Book 2018/00019. Department for Energy and Mining, South Australia, Adelaide, pp. 18–19.
- Pawley M, Wise TW, Dutch R, Spaggiari C, Thiel S and Holzschuh J 2018. What the 13GA-EG1 Eucla-Gawler Seismic Survey tells us about the Coompana Province. In R Dutch, T Wise, M Pawley and A Petts eds, *Coompana Drilling and Geochemistry Workshop 2018 extended abstracts*, Report Book 2018/00019. Department for Energy and Mining, South Australia, Adelaide, pp. 109–119.
- Pawley M, Wise TW, Jagodzinski EA, Dutch R, Tylkowski L, Lockheed A and McAlpine SRB 2018. Coompana Drilling Project: basement lithologies and structure. In R Dutch, T Wise, M Pawley and A Petts eds, *Coompana Drilling and Geochemistry Workshop 2018 extended abstracts*, Report Book 2018/00019. Department for Energy and Mining, South Australia, Adelaide, pp. 52–65.
- Pollard PJ 1989. Geochemistry of granites associated with tantalum and niobium mineralization lanthanides, tantalum and niobium. In P Möller, P Černý and F Saupé eds, *Lanthanides, Tantalum and Niobium: Mineralogy, Geochemistry, Characteristics of Primary Ore Deposits, Prospecting, Processing and Applications Proceedings of a workshop in Berlin, November 1986*, Special Publication 7. Society for Geology Applied to Mineral Deposits, pp. 145–168.
- Roman A and Jaupart C 2016. The fate of mafic and ultramafic intrusions in the continental crust. *Earth and Planetary Science Letters* 453:131–140.
- Shaw DM 1968. A review of K-Rb fractionation trends by covariance analysis. *Geochimica et Cosmochimica Acta* 32(6):573–601.
- Shell Co. of Australia Ltd 1983. EL 747, EL 748 and EL 749, Bunabie Rockhole, Hughes and Nullarbor Plain, progress reports and final report for the period 20/10/80 to 19/10/82, Open file Envelope 04046. Primary Industries and Resources South Australia, Adelaide.
- Smithies RH, Howard HM, Evins PM, Kirkland CL, Kelsey DE, Hand M, Wingate MTD, Collins AS, Belousova E and Allchurch S 2010. *Geochemistry, geochronology and petrogenesis of Mesoproterozoic felsic rocks in the western Musgrave Province of central Australia, and implication for the Mesoproterozoic tectonic evolution of the region*, Report 106. Geological Survey of Western Australia, Perth.
- Smithies RH, Spaggiari CV, Kirkland CL, Wingate MTD and England RN 2015. Madura Province: geochemistry and petrogenesis. In CV Spaggiari and RH Smithies, comps, *Eucla basement stratigraphic drilling results release workshop: extended abstracts*, Record 2015/10. Geological Survey of Western Australia, Perth, pp. 17–28.
- Spaggiari CV and Smithies RH comps 2015. *Eucla basement stratigraphic drilling results release workshop: extended abstracts*, Record 2015/10. Geological Survey of Western Australia, Perth.
- Spaggiari CV, Kirkland CL, Smithies RH and Wingate MTD 2012. What lies beneath - interpreting the Eucla basement. *GSWA 2012 extended abstracts: promoting the prospectivity of Western Australia*, Record 2012/2. Geological Survey of Western Australia, Perth, pp. 25–27.
- Swain G, Barovich KM, Hand M, Ferris GM and Schwarz M 2008. Petrogenesis of the St Peter Suite, southern Australia: arc magmatism and Proterozoic crustal growth of the South Australian Craton. *Precambrian Research* 166:283–296.
- Thiel S, Wise TW and Duan J 2015. Eucla MT profile and modelling. In RA Dutch, MP Pawley and TW Wise eds, *What lies beneath the western Gawler Craton? 13GA-EG1E Seismic and Magnetotelluric Workshop 2015*, Report Book 2015/00029. Department of State Development, South Australia, Adelaide, pp. 49–58.
- Thiel S, Wise TW and Duan J 2018. Electrical signatures of the Coompana Province from AusLAMP and profile MT data. In R Dutch, T Wise, M Pawley and A Petts eds, *Coompana Drilling and Geochemistry Workshop 2018 extended abstracts*, Report Book 2018/00019. Department for Energy and Mining, South Australia, Adelaide, pp. 120–130.

- Travers D 2015. Geochronology and petrogenesis of mafic magmatism in the Coompana Province. Hons thesis, University of Adelaide.
- Wade BP, Payne JL, Hand M and Barovich KM 2007. Petrogenesis of ca 1.50 Ga granitic gneiss of the Coompana Block: filling the 'magmatic gap' of Mesoproterozoic Australia. *Australian Journal of Earth Sciences* 54(8):1089–1102.
- Wingate MTD, Kirkland CL, Spaggiari CV and Smithies HR 2015a. U-Pb geochronology of the Forrest Zone of the Coompana Province. In CV Spaggiari and RH Smithies comps, *Eucla basement stratigraphic drilling results release workshop: extended abstracts*, Record 2015/10. Geological Survey of Western Australia, Perth, pp. 37–40.
- Wingate MTD, Kirkland CL, Spaggiari CV and Smithies HR 2015b. U-Pb geochronology of the Madura Province. In CV Spaggiari and RH Smithies comps, *Eucla basement stratigraphic drilling results release workshop: extended abstracts*, Record 2015/10. Geological Survey of Western Australia, Perth, pp. 14–16.
- Wingate MT, Pirajno F and Morris PA 2004. Warakurna Large Igneous Province: a new Mesoproterozoic large igneous province in west-central Australia. *Geology* 32:105–108.
- Wise TW, Pawley MJ and Dutch RA 2015. Preliminary interpretations from the 2015 Coompana aeromagnetic survey. *MESA Journal* 79:22–30. Department of State Development, South Australia, Adelaide.
- Wise TW, Pawley M and Dutch R 2018a. Interpreted geology map of the eastern Coompana Province. In R Dutch, T Wise, M Pawley and A Petts eds, *Coompana Drilling and Geochemistry Workshop 2018 extended abstracts*, Report Book 2018/00019. Department for Energy and Mining, South Australia, Adelaide, pp. 102–108.
- Wise TW, Pawley M and Dutch R comps 2018b. *Interpreted geology of the eastern Coompana Province*, Special Map, 1:500,000 scale, DIGIMAP 00092. Preliminary edn. Geological Survey of South Australia, Adelaide.
- Wise TW and Thiel S 2018. Imprints of Archean-Proterozoic tectonic processes imaged by magnetotellurics and seismic reflection. In First Australasian Exploration Geoscience Conference, 18-21 February 2018, Sydney Australia, Abstracts. *Preview* 192:121.
- Zaraisky GP, Korzhinskaya V and Kotova N 2010. Experimental studies of Ta₂O₅ and columbite-tantalite solubility in fluoride solutions from 300 to 550°C and 50 to 100 MPa. *Mineralogy and Petrology* 99(3):287–300.

FURTHER INFORMATION

Tom Wise
Tom.Wise@sa.gov.au

Mineral and Energy Resources

Department for Energy and Mining

CHIEF EXECUTIVE

Paul Heithersay
Paul.Heithersay@sa.gov.au
Phone: +61 8 8303 2298

INQUIRIES

Level 4, 11 Waymouth Street,
Adelaide SA 5000
GPO Box 320, Adelaide SA 5001
DEM.MERCustomerServices@sa.gov.au
Phone: +61 8 8463 3000

SOUTH AUSTRALIA DRILL CORE REFERENCE LIBRARY

David Groom
GPO Box 1264, Adelaide SA 5001
David.Groom@sa.gov.au
Phone: +61 8 8379 9574

OPAL FIELDS

Coober Pedy
Ashley Wood
TAFE campus, Hutchison Street
PO Box 475
Coober Pedy SA 5723
Ashley.Wood@sa.gov.au
Phone: +61 8 8672 5800

Mineral Resources Division

EXECUTIVE DIRECTOR

Alex Blood
Alexandra.Blood@sa.gov.au
Phone: +61 8 8429 2478

DEPUTY EXECUTIVE DIRECTOR; MINERAL TENEMENTS and EXPLORATION

Pru Freeman
Pru.Freeman@sa.gov.au
Phone: +61 8 8429 2479

GEOLOGICAL SURVEY of SOUTH AUSTRALIA

Rohan Cobcroft
Rohan.Cobcroft@sa.gov.au
Phone: +61 8 8429 2451

MINING PROJECTS

Martin Reid
Martin.Reid@sa.gov.au
Phone: +61 8 8429 2518

MINING REGULATION

Greg Marshall
Greg.Marshall@sa.gov.au
Phone: +61 8 8429 2472

RESOURCE INFORMATION

Charles Moore
Charles.Moore@sa.gov.au
Phone: +61 8 8429 2477

RESOURCE POLICY AND ENGAGEMENT

Lachlan Pontifex
Lachlan.Pontifex@sa.gov.au
Phone: +61 8 8429 3229

MINING REGISTRAR

Junesse Martin
Junesse.Martin@sa.gov.au
Phone: +61 8 8429 2487

Energy Resources Division

EXECUTIVE DIRECTOR

Barry Goldstein
Barry.Goldstein@sa.gov.au
Phone: +61 8 8429 2449

ENGINEERING OPERATIONS

Michael Malavazos
Michael.Malavazos@sa.gov.au
Phone: +61 8 8429 2470

GEOSCIENCE and EXPLORATION

Elinor Alexander
Elinor.Alexander@sa.gov.au
Phone: +61 8 8429 2436

RESOURCE ROYALTIES AND COMMERCIAL

Nick Panagopoulos
Nick.Panagopoulos@sa.gov.au
Phone: +61 8 8429 2433

Resources Infrastructure and Investment Task Force

Peter Bradshaw
Peter.Bradshaw@sa.gov.au
Phone: +61 8 8429 2991



Follow us @DEM_sagov
https://twitter.com/DEM_sagov



Energy and Mining

<https://www.youtube.com/channel/UCUkhdN2gH4Yi5JYAfQ4aHXQ>

www.energymining.sa.gov.au

www.energymining.sa.gov.au/minerals

www.energymining.sa.gov.au/petroleum

map.sarig.sa.gov.au

www.energymining.sa.gov.au/mesa_journal